DNA-Mediated Charge Transfer in Biological Contexts

Research Report and Propositions

Submitted in Partial Fulfillment of the Requirements for for the Degree of Masters in Chemistry

Anand Vadehra

California Institute of Technology
January 31, 2003

I. Introduction

1. DNA-Mediated Charge Transfer (DNA-CT)

For many years, scientists debated whether DNA was an insulator or a wire (Netzel, 1998; Turro and Barton, 1998). Recent experiments have demonstrated that DNA can, in fact, conduct charge and that it does go through its π-stacked array of nucleobases in a stacking dependent manner (Hall and Barton, 1997; Nunez and Barton, 2000).

Not only is charge transfer in DNA a reality, but it can occur over distances of up to 200 Å! (Nunez et al, 1999). Unlike protein electron transfer, for instance, a shallow distance dependence, though highly debated, has been found (Barton, 1998). Sequence, however, does seem to modulate DNA-CT (Williams et al, 2000). Currently, there are a small handful of plausible theories regarding the mechanism(s) of DNA-CT thriving in the literature (Giese et al, 1999; Bixon et al, 1999; Meggers et al, 1998; Beratan et al, 1998; Lewis et al, 2001)

In order to use DNA as a charge bridge, an electron must initially either be pulled out or put in by an oxidant or reductant. In the case of the oxidant, its oxidation potential must be higher than that of components of the DNA. Of the natural nucleobases, guanine has the lowest oxidation potential (1.29 V) and is, therefore, the most energetically predisposed to lose an electron (support an cation radical, i.e. a positive hole) (Steenken and Jovanovic, 1997). The guanine radical (-H+) is relatively long-lived and susceptible to forming damage products such as 8-oxodG through reaction with H_2O or O_2 (Jovanovic and Simik, 1989). More interestingly, if a guanine is next to another guanine in a DNA sequence, the 5'-G has an even lower oxidation potential. This is due to a greater electron density on the 5'-G in the highest occupied molecular orbital (HOMO) of the 5'-GG-3' dinucleotide, as revealed by theoretical calculations (Sugiyama and Saito, 1996). This reactivity is thought to lead to mutations (and eventually cancer) in the

p53 tumor suppressor gene via 5'-GG-3' and analagous 5'-GGG-3' oxidation hot spots (Kawanishi et al, 2001) as well as 5'-G damage in 5'-GGG-3' containing telomeric DNA repeats, hurrying the aging process (Zhao and Zheng, 2000). As of yet, there is no definitive evidence this type of damage is occurring through DNA-CT *in vivo*.

2. DNA-Protein CT

Despite the above statement, there is precedence for DNA-CT in biological settings. This group has shown that thymine dimers can be repaired by a non-enzymatic one-electron oxidation via DNA-CT (Dandliker et al, 1997). In addition, methyltransferase, M.H*h*a I, a base flipping enzyme that flips out a cytosine for methylation, can affect the electron DNA-ET phenomenon. While the cytosine is held extrahelically, the enzyme replaces it in the π-stack with a glutamine (Fig. 1), abolishing DNA-ET through this junction. Studies using a mutant form of the enzyme, replacing glutamine with the indole-containing tryptophan, showed that DNA-ET could be restored (Fig. 2) (Wagenknecht et al, 2001). This demonstration argues that DNA could potentially activate or repress processes *in vivo* through it's ability to conduct charge.

Unique about this particular study was the correlation of the DNA damage products to the radicals by which they were produced. Transient absorption spectroscopy was used to successfully characterize the co-existence of guanine and tryptophan radicals. From the transient absorption difference spectrum, the absortion maxima from guanine (390nm, 500nm) and that from trytpohan (510nm) were found (Fig. 3). Additionally, absorption curves at 510nm show the presence of increasing amounts of tryptophan radical with increasing equivalents of tryptophan mutant (Fig. 4).

While transient absorption spectroscopy was to used to look at the damage causing radicals, experiments to look at damage products were carried out using the flash-quench technique.

The flash-quench technique was originally developed for proteins (Chang et al, 1991). It can be applied to DNA-CT as well (scheme 1) (Stemp et al, 1997). In this technique, DNA is mixed with a metal complex such as $[Ru(phen)_2dppz]^{2+}$ and a quencher, such as $Ru(NH_3)_6^{3+}$ to quench the excited state of the Ru-complex. Quenching oxidizes the complex to the 3+ state, now a powerful oxidant (1.6 V vs. NHE). Intercalated into the DNA via its dppz ligand (Fig. 2), the Ru-complex pulls an electron out of the DNA. The resulting cation hole migrates through the DNA until it finds a home on hole-friendly guanines where it is deprotonated to the guanine radical. The

stability of the guanine radical leads to an enhancement of damage products due to the reaction with H_20 or O_2 relative to other bases in the π-stack.

Not only is the guanine radical long-lived and hence prone to damage, but the tryptophan radical formed in the mutant is both slower to form and migrate due to poor π-stacking of the indole ring with the natural nitrogenous bases.

In the same study, distance dependence was also examined by looking at guanine oxidation production and kinetics of guanine cation radical formation in oligos where the protein recognition site was marched out to 34 and 51 Å. No significant distance dependence was found for either radical formation of guanine damage. This study clearly demonstrated how a protein could act an activator or repressor of an electron transfer dependent system. The burning question is "how does nature use this ability?" SoxR, a transcriptional activator utilizing a [2Fe-2S], cluster may provide some clues.

II. SoxR

1. The Sox*RS* Regulon

A. Oxidative Stress

When cells experience high levels of damaging oxidants, a.k.a. *oxidative stress*, they must fight for their lives. In *E. coli*, the genetically encoded responses to such events are the *oxyR* and *soxRS* regulons. Each regulon is a distinct groups of genes transcribed in parallel, though physically separated in the *E. Coli* genome (Walkup and Kogoma, 1989).

The soxRS regulon is induced by superoxide, $O_2^{\cdot -}$. $O_2^{\cdot -}$ can reduce DNA-bound Fe^{3+} to Fe^{2+} which can then reduce powerful oxidants such as H_2O_2, forming $HO^{\cdot}$ (Fenton reaction). The oxyR regulon fights to counter produced H_2O_2 in order to diminish dangerous $HO^{\cdot}$ formation. If these two responses didn't take place, DNA (as well as proteins and lipids) would be battered by $HO^{\cdot}$, as it is a prime target for $HO^{\cdot}$ induced damage.

One of the products of the soxRS regulon is SodA, a Mn-containing superoxide dismutase (SOD). SODs convert $O_2^{\cdot -}$ into H_2O_2. While this may seem to make more potential trouble for biomolecules via the fenton reaction, it actually serves to pass on the problem to catalase. Catalase, one of nature's most efficient enzymes and a product of the oxyR regulon, converts H_2O_2 into H_2O and O_2.

B. SoxRS Regulon Induction

While the soxRS regulon is induced by $O_2^{\cdot -}$, agents that *generate* this reactive oxygen species (ROS) in excess of normal levels are some of its more powerful inducers. Paraquat (methyl viologen), plumbagin and menadione are $O_2^{\cdot -}$ generating regulon inducers as well as

redox-cycling agents (Greenberg et al, 1990). Redox-cycling agents are compounds that divert electrons from NADPH or NADH to O_2, forming $O_2^{\cdot -}$. These compounds not only produce harmful radicals, but interfere with metabolic processes to do so. This cooperative effect makes redox-cycling agents particularly harmful.

It turns out there are many other ways to induce the soxRS regulon; the regulon is, in fact, promiscuous. In addition to oxidants such as $O_2^{\cdot -}$, $NO^{\cdot}$ (Ding and Demple, 2000) and diamide also turn it on. Even antibiotics and organic solvents initiate the soxRS regulon (Nunoshiba and Demple,1993; Nakajima et al, 1995). Clearly, this response must be and is broad enough to cope with many kinds of oxidative stress; not just in response to superoxide production, for which it was named (**Superox**ide **R**esponse). Still, there are other ways to induce the regulon. They will be discussed in the next section.

C. Running the soxRS regulon

The soxRS regulon has a two-tier control hierarchy. SoxR is the master regulator, SoxS is its subordinate (Li and Demple, 1994). SoxR is a 17-KDa protein that forms a homodimer in solution (Wu et al, 1995). Near its NTD is a helix-turn-helix motif thought to take part in DNA binding. Its CTD contains four unusually spaced cysteines that act as ligands to a [2Fe-2S] and has sequence homology to bacterial [4Fe-4S] Ferredoxins (Bradley et al, 1997)

SoxR is a member of the MerR family of transcriptional activators (Hidalgo et al, 1995). Like SoxR, these activators bind their promoters on a palindrome in the spacer region between the -35 and -10 sites (sites of RNA polymerase binding); an unusual place for an activator to do its job. SoxR binds the soxS promoter as a dimer on a 18bp palindrome in a suboptimal 19-bp (17-bp is optimal) spacer (Hidalgo et al, 1997) In order to compensate for these extra base pairs,

the DNA is thought to be compressed and kinked by MerR family regulators upon activation (Outten et al, 1999; Heldwein et al, 2001).

An interesting feature of SoxR binding is that it may be in either the apo (no Fe-S cluster), oxidized or reduced state in order to bind the soxS promoter. In fact, it binds with nanomolar affinities regardless of cluster state (Hidalgo and Demple, 1994). Uniquely, however, SoxR becomes an activator only upon oxidation. Though there is no structural evidence, it is believed that, upon Fe-S oxidation, an allosteric shift in the protein's tertiary structure takes place allowing bound RNA polymerase to begin transcription (Outten et al, 1999; Heldwein et al, 2001)

In other words, the Fe-S cluster is a redox-sensing on-off switch for soxS gene expression. The many routes towards regulon induction mentioned in the last section are all ways to, directly or indirectly, flip the switch.

In order to turn on the regulon under oxidative stress, it must first be off. This can be accomplished either by absence of the Fe-S cluster or presence of the reduced Fe-S cluster. The latter seems more likely *in vivo* as it takes drastic reducing conditions *in vitro* to remove the cluster. How does the cluster stay reduced? *In vitro* this can be done by lowering the potential of the environment below the midpoint redox potential (-285mV free in solution; there is no $E_{1/2}$ of DNA-bound SoxR in the literature) of SoxR. Reducing conditions can be achieved with thiols such as DTT and 2-mercaptoethanol, as well as glutathione (Ding et al, 1996; Ding and Demple, 1998). *In vivo*, however, it was long believed that enzymatic reduction was more likely. In fact, an NADPH-dependent cytochrome C SoxR reductase was recently isolated and may be the primary reductant of the Fe-S cluster *in vivo* (Kobayashi and Tagawa, 1999). Furthermore, regulon induction is $NADPH/NADP^+$ dependent; as this ratio lowers the regulon is induced.

This is an example of how to induce the regulon by interfering with its putative reduction pathway, as opposed to actively oxidizing SoxR. In fact, redox-cycling compounds may be more dangerous due to their consumption of NADPH than their concomitant production of $O_2^{\cdot -}$.

D. More on Regulon Activation

While it is conceivable that some oxidation of SoxR occurs directly via $O_2^{\cdot -}$, it is probably not the predominant mode of activation considering $O_2^{\cdot -}$ is a only a mild oxidant. As mentioned, there are a number of ways to oxidize the cluster. The problem is in understanding the bigger picture behind the mechanisms involved. Are there many different mechanisms or just one or two principle pathways? $NO^{\cdot}$ induces the regulon by nitrosylation of the Fe-S cluster under both aerobic and anaerobic conditions. This works not by an oxidative mechanism, but it's believed that the nitrosylated (Fe-S cluster) protein is structurally similar to the oxidized protein; this common structure is believed to be transcriptionally activating (Ding and Demple, 2000). Still, most mechanisms are thought to occur through oxidation of the Fe-S cluster.

If the redox-switch is sensitive to many different stimuli, could it lose an electron via any other mechanisms? What about indirect electron transfer, i.e. from a distance? This would require a bridge to couple SoxR to its oxidant. Could DNA play this role?
This question led us to pursue the experiments described herein.

2. SoxR-DNA Experiments

In order *to begin* to understand a possible SoxR-DNA electron transfer we needed to define a system in which to work. As opposed to binding SoxR to a long SoxS promoter fragment subcloned into a plasmid, we designed a 33-mer dsDNA oligo containing the 18bp palindromic binding site:

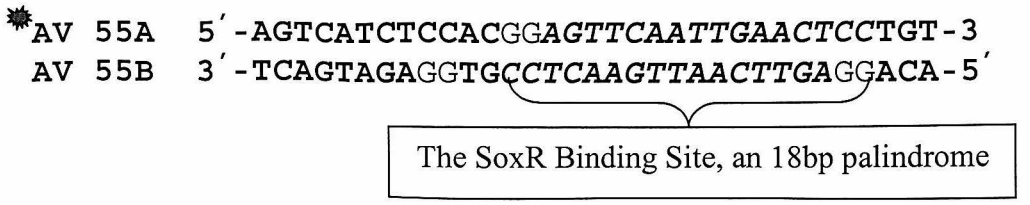

Oligos such as AV55A/B are quick and easy to synthesize by standard solid phase methodologies. In addition, DNA damage from FQ experiments on small oligos can easily by resolved by gel electrophoresis. Also, in order to tether intercalating photo-oxidants for future FQ experiments (to be described), a free 5'-OH is required. Also, tethering is not efficient to oligos over ~35 bases (unpublished observations). This linkage should be in proximity to the SoxR binding site, a requirement met by usage of a short oligo.

It turned out that synthesis of AV55A and AV55B proved more than trivial. Purification by reversed phase HPLC (traces not shown) revealed a variety of amorphous peaks.

There were a few reasons for these convoluted HPLC traces. First, both oligos contained an 18bp palindrome. Mutilple secondary structures, such as hairpins and stem and loops, can form during single stranded purification. Each of these structures shows up as an individual peak. To complicate matters further, dimethoxytrityl (DMT) deprotection from the 5' nucleotide during solid phase synthesis wasn't very efficient with either AV55A or AV55B. This was due to complications that arose when these same alternative structures formed during synthesis, pinning the oligo against itself and partially shielding the DMT group from the acidic solvent, diminishing cleavage. In summary, not only did the HPLC traces reflect multiple secondary structures, but DMT protected and deprotected versions of each. Additional rounds of manual DMT deprotection in tandem with high temperature (60°C) HPLC or DPAGE were both

employed to purify the oligos under denaturing conditions. Either method was able to deconvolute purification by disfavoring the formation of most secondary structures. Maldi-MS was performed on the purified oligos revealing the full length, deprotected strand by mass.

a. Gel Shift Analysis

With AV55A/B in hand, we had first to establish SoxR binding. Gel Shift analysis was used to ascertain the equivalents of SoxR necessary to fully bind AV55A/B. Initial attempts revealed no shift. In addition, each attempt had multiple bands (also in controls). To figure out the problem, the protocol was reviewed thoroughly. The problem, as it turned out, was in the protocol. It called for 250pM AV55A/B.

Originally, this protocol was used for 180bp PCR fragments. With such a long strand, double strand formation can occur at picomolar concentrations. However, AV55A/B wasn't stable at these concentrations (Fig. 5), even in our high salt conditions. To ascertain the concentration at which dsDNA was forming, we scaled up concentrations (5nM-120nM) and viewed 32P-AV55A/B formation by native-PAGE (Fig. 6). As suspected, duplexes were not forming at the previous concentrations. In fact, AV55A/B didn't form predominantly until concentrations of 100-120nM.

A protocol-modiifed gel shift analysis was carried out to gauge binding of SoxR to AV55A/B. After a few attempts to optimize for SoxR binding pre-incubation time, % acrylamide gel and gel running time, a gel shift was observed (Fig. 7).

Results show SoxR was fully bound to AV55A/B at 15 equivalents SoxR dimer as evidenced by the band shift. The experiment was performed with and without 2mM DTT in the SoxR binding buffer. DTT has been shown to stabilize the $[2Fe\text{-}2S]^{2+/1+}$ cluster. However, DTT

is also a good reductant of the guanine cation radical. During guanine oxidation produced by FQ experiments DTT may reduce guanine cation radicals,
diminishing otherwise observed damage.

It's important to note binding was observed with or without DTT. Without DTT, however, it's possible we were observing binding of the apo form. This must be a consideration given that SoxR binds wild type soxS promoter in any of its three forms with similar affinity (K_D=4-40nM).

b. Flash-Quench Experiments

Initial SoxR-DNA FQ experiments proved troublesome. First, we observed SoxR-DNA cross-linking. This disallowed visualization of guanine oxidation due to FQ because piperidine cleavage of the damage products was obstructed where SoxR was bound (Fig 8). Crosslinking was evidenced by the shift of the parent band in all lanes but "no SoxR" (2^{nd} lane from the left). This issue was combated by treatment with proteinase K, a robust serine protease, to the FQ samples following irradiation. Proteinase K would act to chew SoxR off the oligo, leaving it fully exposed for subsequent piperidine treatment. This strategy was successful as seen in a sample gel (Fig. 9) of a FQ experiment using the same procedure and conditions as in Fig 8. The shifted band seen in Fig.8 was absent as the parent bands returned.

Despite solving the cross-linking problem, there was no guanine oxidation observed above controls. Under the high salt conditions required for protein binding, it was conceivable that quencher ($Ru(NH_3)_6Cl_3$ or $Co(NH_3)_5Cl_3$) was out competed by other salts for DNA access.

The next set of FQ experiments were carried out in the absence of SoxR. In this way conditions for guanine oxidation could be secured before usage of the precious SoxR protein

stock. After much experimental optimization with quenchers, quencher concentration and irradiation time and switching from a HgXe arc lamp w/ a monochromator to a HeCd laser as a light source, a successful FQ experiment was conducted. The successful experiment, as visualized by phosphorimagery of the DPAGE gel in Fig. 10, shows a unique guanine damage pattern. As noted earlier, G^{ox} usually occurs exclusively at the 5'G of 5'-GG-3'. The labeled strand, AV55B, contains two 5'-GG-3' sites, one outside the binding site and one at its far end (from the 32P label).

In this experiment, the observed damage pattern was not predicted. Damage occurred at both guanines in both guanine doublets. In addition, guanine damage occurred at the 5' G of the 5'-GAA-3' near the middle of the palindromic binding site. 5'-GAA-3' can be thought of similarly to 5'-GG-3' or 5'-GGG-3'. All are short purine stretches with excellent π-stacking. Just as the HOMO on the 5'G of 5'-GG-3' or 5'-GGG-3' is very large, hence its low oxidation potential, the 5'G of 5'-GAA-3' may also have a large HOMO. But why are both guanines in each guanine doublets also getting damaged? This may also be reconciled by looking at sequence context. Both guanine doublets are part of a 5'-GGAG-3' sequence. While not known for sure, it seems as though a similar thermodynamic effect (i.e. increase in HOMO size) is taking place.

With the FQ cycle established in the absence of SoxR, the same experiment was performed with SoxR. Preliminary experiments showed little effect of SoxR binding (Fig 11). As expected, the only site of damage vulnerable to significant effects from SoxR binding was the 5'G of 5'-GAA-3'. Located near the middle of the palindrome (AV55B), this guanine could be either de-stacked by DNA kinking induced by SoxR binding or better stacked due to DNA rigidification during binding. At the present time, there is no crystal structure of SoxR bound to

DNA, leaving either hypothesis a reasonable possibility. The gel showed a dimunition of about one-half in damage at this site relative to samples without SoxR.

The next goal was to assess the SoxR-DNA FQ cycle with $SoxR_{red}$. SoxR can be reduced chemically, in air, by treatment with sodium dithionite. Binding of $SoxR_{red}$ to DNA should occur with little to no DNA distortion based upon the current DNA kinking hypothesis upon oxidation of SoxR and subsequent transcription of soxS. We'd like to assess the DNA damage pattern with $SoxR_{red}$ vs. $SoxR_{ox}$. If, in fact, we are doing DNA-CT with bound SoxR we might see a distinction in the pattern due to the potential differences in π-stacking as a result of SoxR redox state.In order to test this hypothesis we performed a standard SoxR-DNA FQ experiment (Fig. 12) with the inclusion of 2mM dithionite preincubated for one half-hour with SoxR-DNA pre-FQ. There were a number of striking results from this experiment. First and foremost, the dark controls, "no hv" and "No hv/No Ru-dppz", showed significant damage at the 5'G of the 5'-GG-3' (5'-**G**G-3'). This was an unexpected result. Without irradiation, the FQ cycle should be inactive and therefore no reaction should occur. Yet, the amount of 5'-**G**G-3' damage in the "No hv" sample was comparable to the cases in which the FQ cycle was fully operable, "No Dithionite" (i.e. $SoxR_{ox}$) and "All" (i.e. $SoxR_{red}$). Did light leak in, i.e. was this result a consequence of allowing stray ambient light (outside the dark, laser room) to induce the FQ cycle? The amount of 5'-**G**AA-3' damage for this sample indicates the answer is no because it is at the same level of the other (non-FQ conditions) controls, "No hv" and "No hv/No Ru-dppz", 2.5-4.5 fold lower than the FQ samples. In other words, if the damage in the "No hv" sample was due to FQ-induced DNA-CT based damage, *both* the 5'-**G**G-3' and the 5'-**G**AA-3' damage levels would be above controls.

Comparison of the "No hv/No Ru-dppz" and "No Ru-dppz" samples show similar levels of 5'-**G**G-3' damage. Therefore, damage appears to be light-independent with even higher levels upon addition of Ru-dppz ("No hv" sample). Inspection of the "No SoxR" and "No SoxR/No Dithionite" samples show a decrease in 5'-**G**G-3' relative to all other samples. The 5'-**G**AA-3' damage in these samples, however, were higher than the levels in any of the controls (No hv, No hv/No Ru-dppz, No Ru-dppz). This damage and the overall damage pattern in the "No SoxR" samples was reflective of the FQ-induced (DNA-CT) damage pattern observed in previous gels (Figs. 10,11) without SoxR.

Still, an important question is how the 5'-**G**G-3' damage in the "no hv" sample is generated compared to the "no dithionite" and "all" samples. In order to answer this question, we performed a series of experiments, most of which were dark controls. We hoped to find the source of the high levels of 5'-**G**G-3' damage in "No hv" sample.

An answer to this question is found in Fig. 14. Amazingly, the only component needed to induce DNA damage over background (lane 1) at the 5'-**G**G-3' was SoxR (lane 2). This was accomplished simply by incubating $SoxR_{ox}$ with DNA for 1.5 hours (1/2 hour for binding, 1hour to simulate irradiation time) at room temperature in the dark. Addition of dithionite to make $SoxR_{red}$ led to a slight attenuation in damage (lane 3). Incubation with Ru-dppz and/or quencher with either $SoxR_{ox}$ or $SoxR_{red}$ (lanes 4-9) led to a further reduction in damage (compared to lanes 2 and 3). Conversely, SoxR-DNA FQ reactions produced the expected damage pattern (lanes 10 and 11).

What are the different damage patterns telling us? Inspection of Figs. 12 and 14 seems to be telling us that the damage pattern observed for SoxR-DNA FQ (Fig. 12, "No Dithionite", "All"; Fig. 14, lanes 10 and 11) reactions is a composite of the damage observed with SoxR-less

DNA FQ reactions (Fig. 12, "No SoxR", "No SoxR/No Dithionite") and spontaneous reaction during SoxR-DNA binding (Fig. 14, lanes 2 and 3). In other words, the FQ-induced damage pattern observed without SoxR is present with SoxR "bound" because it represents damage to DNA not actually bound by SoxR. Likewise, the enhancement in FQ-induced damage at the 5'-GG-3' site with SoxR versus without SoxR must be due to a mechanistically distinct redox reaction occurring between the SoxR and DNA. In addition, it appears as though SoxR's palindromic DNA-binding site is not damaged by SoxR binding (Fig. 14, both AV55A and AV55B), rather damage occurs only outside the binding site (5'-**G**G-3' on 32P-AV55B). But how is SoxR damaging the 5'-**G**G-3' located 2 bp outside its binding site?

A first guess might be that free Fe^{2+} dissociated from SoxR reacts with peroxides (possibly from Tris buffer) to form hydroxyl radicals (Fenton-type chemistry), known DNA damage agents. However, hydroxy radicals would cause indiscriminate damage on the DNA bases. Instead, we see damage solely at the 5'-**G**G-3', a trademark of DNA-CT based damage.

Another possibility is that the SoxR $[2Fe\text{-}2S]^{2+/1+}$ can touch the 5'-**G**G-3', damaging it via direct oxidation. This notion could be supported by the fact that $SoxR_{red}$ caused slightly less damage than $SoxR_{ox}$ (compare lanes 3 and 2, Fig. 14). The location of the Fe-S clusters in $SoxR_{dimer}$, however, are unknown at the present time.

A final possibility is that the protein is electronically coupled into the π stack (probably via an intercalating aromatic side chain which would also stabilize binding; based on the homologous BmrR, DNA-bound structure this makes sense (Heldwein and Brennan, 2001)) and spontaneously, reversibly oxidizes the DNA. But why would $SoxR_{ox}$ want to oxidize DNA? It probably doesn't. In *E. coli*, the protein is presumably kept in the reduced form. Therefore, an oxidation of DNA *in vivo* is unlikely. However, what if the DNA oxidation we witnessed was an

artifact of experimental conditions, i.e. we were using mostly $SoxR_{ox}$. In other words, if SoxR can reversibly oxidize DNA, by definition, it can reduce it. Therefore, might the damage seen in Fig. 14, lane 2, originate from spontaneous oxidation of the 5'-**G**G-3' via DNA-CT, while slightly lower damage with $SoxR_{red}$ (Fig. 14, lane 3) can be attributed to the inability of $SoxR_{red}$ to oxidize or even the ability to reductively repair of oxidation of DNA somehow generated *in situ*.

Using this last scenario, what are the implications of this spontaneous redox chemistry upon binding of SoxR? Consider $SoxR_{red}$ (physiogically relevant inactive state) bound to its palindromic binding site in the soxS promoter. Imagine the bacteria is invaded by oxidants (oxidative stress). What happens next? How does SoxR respond? If $NADPH^+$ is indiscriminantly consumed by the oxidative environment, depleting reduction equivalents for SoxR, might SoxR autooxidize, turning on the SoxRS regulon to counter the oxidative stress? Possibly. In fact, this may be an important activation mechanism *in vivo*. Consider, however, an alternative situation.

It is known that many of the oxidants that stimulate regulon activity also damage DNA. It also known from studies in our lab and many others that the 5'-G of 5'-GG-3' has an especially low oxidation potential and, therefore, is one of the predominant sites of oxidative damage in genomic DNA.

Upon oxidation of DNA via oxidative stress, 5'-**G**G-3' is "sensed" by $SoxR_{red}$ (Fig. 16). In this model, SoxR, coupled to the soxS promoter DNA through an intercalating aromatic amino acid, reductively repairs the newly formed guanine cation radical via DNA-CT, i.e. autooxidizes. In turn, the soxRS regulon is switched on and oxidative stress is combated. In our model system, we have a 5'-GG-3' located 2 bp upstream of the binding site. The wild-type soxS promoter also

has a 5'-GG-3' located upstream of the binding site. While this distance is 15 bp, far more than 2 bp, it remains well within the distance regime of efficient DNA-CT.

3. SoxR-DNA EPR Experiments

FQ/EPR and non-FQ, SoxR-DNA interaction EPR experiments can help us look at the SoxR's $[2Fe\text{-}2S]^{2+/1+}$, the next step in understanding SoxR-DNA ET. In the reduced state, an EPR signal with three distinct g values is known for SoxR (Hidalgo et al, 1997). Conversely, the oxidized (and apo) state are not EPR active. For these reasons, FQ/EPR allows us to look at direct ET between our Ru-complexes and the SoxR Fe-S cluster or via DNA, if this occurs. Alternatively, EPR of the non-FQ, SoxR-DNA interaction could help us in assessing any changes in redox state that might occur upon SoxR binding and "sensing" of damage (Fig. 16). At this point, only (preliminary) FQ/EPR (no non-FQ) experiments have been performed. These experiments were carried out the same way as SoxR-DNA FQ experiments. The crucial difference was that the DNA was not radioactively labeled.

The "No hv" sample had $SoxR_{red}$ (from treatment w/2 mM dithionite) and all FQ components except it was not irradiated. Therefore, we should observe an EPR signal from this sample. On the other hand, all other samples either lack SoxR, dithionite, or were exposed to operable FQ conditions. Therefore, if photoinduced, FQ-driven, Fe-S cluster oxidation via DNA-CT can occur, samples other than "No hv" should have a bleached or diminished EPR signal in comparison. In reality, the signal should probably be diminished only because SoxR is in 15:1 excess with respect to the DNA and, therefore, a large percentage of the chemically reduced SoxR was not DNA bound and therefore would not participate. In the future, this ratio will be decreased by increasing the amount of DNA.

While not yet optimized, some interesting results have been observed. As shown in Fig. 17a., the signal/noise of the EPR spectra of a SoxR-DNA FQ experiment was low making it difficult to rationalize the results. However, inspection of the "No hv" sample alone reveals the existence of a small signal among the noise (Fig. 17b). Integration of all signals reveals this distinction more clearly (Fig. 18). These spectra correspond to actual EPR absorptions. Usual EPR spectra (Fig. 17) are first derivatives of the absorption spectra and are used because they reveal identifying peak shape information less distinguishable in the absorbance spectra.

Fig. 18 shows a distinct absorption for $g_{//}$=1.93, characteristic of $[2Fe\text{-}2S]^{1+}$ clusters. None of the other samples have this peak. This means one of two things. First, in the "All" or "No DTT" (DTT is thought to aid in cluster stability, but may not be necessary) sample, we might be looking at a loss of signal due to cluster oxidation. Alternatively, as in the case with the remaining samples, we may be looking at the apo-SoxR (EPR equiv. to "No SoxR"). Whether we observed an oxidized cluster as a result of FQ or simply the apo-form from oxidative degradation has yet to be determined. Nevertheless, the results are intriguing and will be repeated under optimized conditions. Once these are worked out, further experiments employing both tethered and non-tethered Ru-dppz complexes, under aerobic and anaerobic conditions will be performed. First and foremost, however, we will explore the model proposed in Fig. 16. using these same considerations.

There are a variety of experiments we can do to validate our model (rather disprove alternative models). First, we will perform non-FQ, SoxR-DNA interaction experiments with apo-SoxR. According to our model, this would prevent damage to the 5'-**G**G-3'. Assuming our damage is abolished, we will then synthesize an oligo that contains a larger fragment of the wt-soxS promoter (including the 5'-GG-3' 15 bps upstream of the SoxR binding site. We will

perform the same experiment as with the shorter oligo and assess 5'-GG-3' damage. If damage is abolished, the mechanism may be through a direct interaction between the DNA and the Fe-S cluster. If it is the same or slightly diminished, its probably occuring via DNA-CT.

4. Flash Quench/Transient Absorption Spectroscopy (FQ/TAS)

Transient absorption spectroscopy (TAS), discussed earlier, will be used to look at the radicals generated as result of Ru-dppz photo-excitation and quenching (FQ/TAS). Quenching of our excited state Ru-complexes results in powerful oxidants. This leads to oxidative damage to the electronically coupled DNA bases. While the long-lived guanine radical can be characterized using TAS, recall that an aromatic protein moiety intercalated into the π-stack is vulnerable to DNA damage as well. In fact, the TAS absorption spectrum for both the tyrosine and tryptophan cation radicals has been determined by this group (Wagenknecht et al, 2000).

In the case of SoxR-bound DNA, there is no evidence of specific DNA contacts. However, the related activator BmrR, has been structurally characterized by x-ray crystallography and shown to have tyrosines on either end of the palindrome in van der waals contact with the ring system of a guanine and an adenine (Heldwein and Brennan, 2001). At least in this related example, there is plausibilty to not only electronically couple the DNA to its bound protein, but to characterize the radical (tyrosine) which would first form in the DNA-protein electron exchange. Whether spontaneous autooxidation of SoxR's $[2Fe\text{-}2S]^{2+/1+}$ cluster (non-FQ) or FQ-based oxidation occurs (or neither), TAS should help understand the mechanistic details.

As in other experiments, FQ/TAS and non-FQ/TAS experiments will involve aerobic, anaerobic, tethered and non-tethered conditions. These experiments will correlate damage

patterns seen in FQ or non-FQ experiments to the radicals responsible for this damage under the same conditions. In fact, through observation of an aromatic side chain radical, it can be concluded that the DNA and protein are electronically coupled.

Prior experiments at this juncture will have served to answer a number of questions. First, what is the charge transfer ability of DNA with bound SoxR in its various states? Second, can we witness an oxidation change in the SoxR Fe-S cluster via any of the described FQ conditions? Third, can we see protein radical formation while bound to soxS promoter DNA? Finally, can we change the SoxR Fe-S cluster oxidation state via DNA-CT?

Having answered these questions, we will attempt to make functional use of our new knowledge. Given that regulon induction occurs with SoxR oxidation, we will devise a transcriptional assay to determine if we can turn on soxS transcription at a distance, via DNA-CT, either via the FQ technique or simple incubation of SoxR with DNA (non-FQ).

Previous *in vitro* transcriptional assays of soxS have used a soxS promoter containing plasmid (e.g. *pBD100*), incubated with RNA polymerase, and looked for primer extension products of the soxS gene by gel electrophoresis (Hidalgo and Demple, 1997). Additionally, *in vivo* and *in vitro* assays have used soxS::*lac z* fusions in which β-galactosidase (the lac z gene product) activity is monitored to determine transcriptional activity (Hidalgo and Demple, 1994). Control *bla* gene transcripts were used in the first case to examine soxS transcription levels due to oxidized SoxR.

Our transcriptional assay(s) will be based on these established protocols. In order to do non-FQ in *vitro* experiments or FQ experiments with non-tethered $[Ru(phen)_2ddpz]^{2+}$, we may use any of these setups. However, our system using tethered $[Ru(phen)bipy'(dppz)]^{2+}$ demands greater preparation. Coupling of DNA to a metal complex via a tether is not efficient on long

oligos (≥35). Additionally, coupling must occur at a free 5' end. As a result, an alternative methodology must be employed to tether our metal complex to soxS DNA. SoxRS locus-containing plasmid *pBD100* will be digested with BamH1 and EcoR1 to yield a 149bp soxS promoter-containing sticky-ended restriction fragment. This segment will then be ligated to a short oligo with a Ru-modified blunt end and an EcoR1 sticky end (Scheme 2). This fragment will be subcloned into a *pBR322* derived vector containing the *lac operon* genes via ligation of BamH1 sticky ends and will allow us to create a *soxS'::lacZ operon* fusion. The plasmid will remain linearized due to the 5' end tether. The plasmid has an inserted *kan* gene for selection purposes (part of the tet gene will be removed in order to insert 149bp segment). With the lac genes under control of the soxS promoter, we will now have the ability to assay soxRS regulon induction via DNA-CT through standard B-galactosidase activity detection.

Lastly, a natural redox active cofactor (e.g. riboflavin) could be substituted for our Ru-complex in our FQ-based transcription assay to further assess the plausibility of the DNA-ET Fe-S oxidation mechanism in vivo.

To make this point clear, the need to tether (or even use) in order to do FQ may be unnecessary if, in fact, SoxR is autooxidized in response to G^{ox} at the 5'-GG-3' 15 bp upstream of the SoxR binding site

III. MutY

1. Background

MutY is a DNA base excision repair (BER) enzyme. An adenine glycosylase, MutY flips out and cleaves adenines mispaired with guanines or 8-oxoguanines (OG). This action helps prevent G:C→A:T transversions during replication (David, 1998b).

MutY is comprised of a CTD and an NTD (containing a [4Fe-4s] cluster). The NTD, aka Stop225, is known to be catalytically active, only less discriminate in its preference for OG:A over G:A substrates as compared with wt-MutY (David, 1998a).

The kinetics of the reaction with mispaired DNA are known to be biphasic, a burst phase followed by a slower phase. The slow phase has been attributed to the adenine cleavage reaction while the slow phase is due strong product binding (i.e. slow product release). Slow release is thought to be a protection mechanism for the apurinic DNA after the action of MutY. Protection is believed to occur until MutM or other related repair proteins takes the DNA to remove the G or OG from the opposite strand (David, 1998a).

2. Preliminary EPR Experiments

Our interest in MutY stemmed from our general curiosity concerning metal containing, DNA repair and regulatory, DNA-binding proteins and DNA-CT. Preliminary EPR experiments with MutY and 21-mer oligos have provided some intriguing results.

The experiment was straightforward. We mixed MutY and DNA together for varying periods of time, froze the mixture in a dry ice/acetone bath (196 K) or liq. N_2 (77 K) and then took their EPR spectra at 77 K.

EPR experiments using all AT 21mers ($d(AT)_{21}$) demonstrated the growth of a signal over time (Fig. 19). This phenomenon has been found upon mixing MutY with DNA, but not with either alone. This is a distinctly important fact considering the experiments contained $(AT)_{21}$. The EPR signal, therefore, should be attributed to a protein-associated radical. The DNA contains no guanines, the easiest base with which to form radicals. Hence, radical

formation in all AT sequences is not expected to be stable. There is no certainty as to whether the radical is amino acid-derived or from the [4Fe-4S] cluster or both.

Performed numerous times, the experiment with an all AT oligo (Fig. 19) showed little repeatability in signal growth trend. In this example, the signal maximized at 40 minutes, decreased at 60 minutes and went up slightly at 80 minutes. In Figs. 20 and 21, EPR spectra of an experiment using a mismatched oligo, the signal was weak until it darted up and maximized at 80 minutes. This result is potentially remarkable considering the presence in this experiment of a mismatch substrate.

If, in fact, a protein-radical is formed upon MutY binding to DNA in the all AT strands, why is it attenuated when bound to mismatched DNA? Is radical formation part of some scanning mechanism by the repair protein searching for mispairs? Might we be seeing inconsistent EPR signal growth trends in the experiments with all AT DNA because we're only taking EPR "snapshots", viewing random, varying population distributions of DNA-bound and free MutY? On the other hand, could protein radical formation be quenched during adenine glycosylase activity, only to shoot up upon completion of repair, creating a situation analogous to having all AT sequences (i.e. no mismatches)?

In order to associate the observed EPR signals with the hypothesized "scanning" and repair of DNA by MutY, a glycosylase activity DPAGE experiment was carried out. The experiment employed the protocol used by S.S. David to follow enzyme activity over time (David, 1998a). In this experiment, the DNA strand containing the cleavage-vulnerable adenine was radiolabeled on its 5' end using ^{32}P-ATP. MutY was mixed with the dsDNA oligo. Aliquots were removed at given time intervals (1-120 min) and quenched and cleaved at the

newly formed abasic site by addition of NaOH. Samples were loaded onto DPAGE gels and visualized by phosphorimagery.

Parallel reactions were run for samples with or without BSA. BSA is believed to increase MutY stability in air and therefore, allow longer periods for aerobic *in vitro* glycosylase activity studies. We were curious to see if this effect was small enough not ignore because we believe our EPR spectra contain contaminating Cu^{2+} traces. BSA binds Cu^{2+} well and could be exacerbating the problem by strengthening the Cu^{2+} EPR signal.

As expected, the visualized gel revealed one parent band (full-length oligo) replaced over time by a shorter band, the length (mobility) of which is 6bp because the G:A mispair (i.e. the cleavage site) is the 7^{th} bp from the 5'end of the labeled strand. The "repair" (growth of shorter strand on gel) maximized at about 60% for samples both with and without BSA (Fig. 22a). We believe this is because our active protein concentration was over estimated and more protein needs to be used for future experiments. This is only an issue because the protein is known to lose functionality in air between 30 and 60 minutes.

As expected, however, the BSA samples maxed out in about half the time (15 min) as the non-BSA samples (30 min). Therefore, if we wanted to avoid using BSA in further experiments we could, confidently, look only at the first 15-20 minutes after MutY-DNA mixing.

Our goal was to compare the shape of the repair curve of a G:A mismatch by MutY to the growth of the observed EPR signal. In Fig.22b, we plotted normalized integrated EPR signal intensity growth and DNA repair by MutY on the same time scale. From this overlay, it is clear that there may be some correlation between the two. Both curves exhibit a similar shape (maxing out, decaying, growing and decaying again) over

similar times. The reason for the eventual decay of the curves has not yet been determined; possibly MutY-bound DNA is precipitating out of solution over time.

Having done these initial experiments, we wanted to look at the effects of oxidants and reductants on this system to see how they might alter EPR signal growth. We used DTT as our reductant and ferricyanide as our oxidant. As seen from Fig. 23, EPR signals of the MutY-DNA interaction were distinctly affected by addition of oxidant or reductant. In these experiments, DTT or Ferricyanide ($Fe(CN)_6$) was either incubated with MutY/DNA at T=0 or for only the last few minutes before freezing. The latter of these two types of experiments were performed to assay whether the EPR signal could be reversibly reduced or stabilized by these additives.

The results were promising (Fig. 24). Addition of DTT at T=0 (known stabilizer of Fe-S clusters), seemed to enhance (the integrated intensity of) EPR signal growth compared to the same experiment without DTT ("MutY-Buffer-DNA"). Conversely, addition of $Fe(CN)_6$ at T=0 attenuated the signal over time compared to the experiment without it ("MutY-Buffer-DNA"). Furthermore, addition of DTT or $Fe(CN)_6$ to the "MutY-Buffer-DNA"sample a few minutes before freezing demonstrated similar effects.

We have looked further into the implications of these results with mutant forms of MutY. Initial experiments (not shown), however, showed no growth of EPR signal above buffer levels. Glycosylase activity experiments will be performed in order to understand these observations.

3. Future Studies on the DNA-MutY Interaction

a. EPR

The initial experiments will be performed again after attempts to remove any Cu^{2+} inpurities. In addition to the oligos already described, experiments will be carried out with oligos containing one G:C (otherwise all AT) as well as experiments on calf-thymus DNA. Additionally, experiments will be performed in the absence of oxygen and at lower temperatures.

V. References

Barton, J. K. (1998) *Pure Appl. Chem.* **70**:873-879.
Beratan, D. N.; Skourtis, S. S. (1998) *Curr. Opin. Chem. Biol.* **2**:235-243.
Bixon, M.; Giese, B.; Wessely, S.; Langenbacher, T.; Michel-Beyerle, M. E.; Jortner, J. (1999) *Proc. Natl. Acad. Sci.* **96**:11713-11716.
Bradley, T. M.; Hidalgo, E.; Leautaud, V.; Ding, H.; Demple, B. (1997) *Nuc. Acids Res.* **25**:1469-1475.
Chang, I. J.; Gray, H. B.; Winkler, J. R. (1991) *J. Am. Chem. Soc.* **113**:7056
Dandliker, P. J.; Homlin, R. E.; Barton, J. K. (1997) *Science.* **275**:1465-1468
David, S.S. (1998a) *Biochemistry* **37**:14756-14764
David, S.S. (1998b) *Biochemistry* **37**:6465-6475
Ding, H.; Demple, B. (1998) *Biochem.* **37**:17280-17286.
Ding H.; Demple, B. (2000) *Proc. Natl. Acad. Sci.* **97**:5146-5150.
Ding, H.; Hidalgo, E.; Demple, B. (1996) *J. Biol. Chem.* **271**:33173-33175.
Gaudu, P., Dubrac, S.; Touati, D. (2000) *J. Bacteriol.* **182**:1761-1763.
Gaudu, P.; Weiss, B. (1996) *Proc. Natl. Acad. Sci. USA* **93**:10094-10098.
Giese, B.; Wessely, S.; Spormann, M.; Lindemann, U.; Meggers, E.; Michel-Beyerle, M. E. (1999) *Angew. Chem. Int. Ed.* **38**:996-998.
Greenberg, J. T.; Demple, B. (1989) *J. Bacteriol.* **171**:3933-3939.
Greenberg, J. T.; Monach, P.; Chou, J. H.; Josephy, D.; Demple, B. (1990) *Proc. Natl. Acad. Sci. USA* **87**:6181-6185.
Hall, D. B.; Barton, J. K. (1997) *J. Am. Chem. Soc.* **119**:5045-5046.
Heldwein, E. E. Z.; Brennan, R. G. (2001) *Nature* **409**:378-382.
Hidalgo, E.; Bollinger, J. M.; Bradley, T. M.; Walsh, C. T.; Demple, B. (1995) *J. Biol. Chem.* **270**:20908-20914.
Hidalgo, E.; Demple, B. (1994) *EMBO Jour.* **13**:138-146.
Hidalgo, E.; Demple, B. (1997) *EMBO J.* **16**(5):1056
Hidalgo, E.; Ding, H.; Demple, B. (1997) *Cell*, **88**:121-129.
Holmlin, E.R.; Dandliker, P.J. & Barton, J.K. (1999) *Bioconjug. Chem.* **10**:1122
Jovanovic, S. V.; Simic, M. G. (1989) *Biochim. et Biophys. Acta.* **1008**:39-44.
Kawanishi, S.; Hiraku, Y.; Oikawa, S. (2001) *Mut. Res.* **488**:65-76.
Kielkopf, C.L.; Erkkila, K.E.; Hudson, B.P.; Barton, J.K.; Rees, D.C. *Nat. Struc. Biol.***7**:117
Kobayashi, K.; Tagawa, S.(1999) *FEBS Letters* **451**:227-230.
Lewis, F. D.; Letsinger, R. L.; Wasielewski, M. R. (2001) *Acc. Chem. Res.* **34**:159-170.
Li, A.; Demple, B. (1994) *J. Biol. Chem.* **269**:18371-18377.
Meggers, E.; Michel-Beyerle, M. E.; Giese, B. (1998) *J. Am. Chem. Soc.* **120**:12950-12955.
Nakajima, H. K.; Kobayashi, H.; Aono, R.; Horikoshi, K. (1995) *Biosci. Biotechnol. Biochem.* **59**:1323-1325.
Netzel, T. L. (1998) *J. Biol. Inorg. Chem.* **3**:210-214.
Nunez, M. E.; Hall, D. B.; Barton, J. K. (1999) *Chem. & Biol.* **6**:85-97.
Nunez, M. E.; Barton, J. K. (2000) *Curr. Opin. Chem. Biol.* **4**:199-206.
Nunoshiba, T.; Demple, B. (1993) *Cancer Res.* **53**:3250-3252.
Outten, C. E.; Outten, F. W.; O'Hallora, T. V. (1999) *J. Biol. Chem.* **274**:37517-37524.
Prat, F.; Houk, K. N.; Foote, C. S. (1998) *J. Am. Chem. Soc.* **120**:845-846.

Steenken, S.; Jovanovic, S. V. (1997) *J. Am. Chem. Soc.* **119**:617-618.
Stemp, E.D.A.; Arkin, M.R.; Barton, J.K. (1997) *J. Am. Chem. Soc.* **119**: 2921
Sugiyama, H.; Saito, I. (1996) *J. Am. Chem. Soc.* **118**:7063-7068
Touati, D. (2000) *Redox Report* **5**:287-293.
Turro, N. J.; Barton, J. K. (1998) *J. Biol. Inorg. Chem.* **3**:201-209.
Walkup, L. K. B.; Kogoma, T. (1989) *J. Bacteriol.* **171**:1476-1484.
Wagenknecht, H.A.; Stemp, E.D.A.; Barton, J.K. (2000) *Biochemistry*. **39**:5483
Wagenknecht, H.; Rajski, S. R.; Pascaly, M.; Stemp, E. D. A.; Barton, J. K. (2001) *J. Am. Chem. Soc.* **123**:4400-4407.
Williams, T. T.; Odom, D. T.; Barton, J. K. (2000) *J. Am. Chem. Soc.* **122**:9048-9049.
Wu, J., Dunham, W. R. & Weiss, B. (1995) *J. Biol. Chem.* **270**:10323-10327.
Zhao C. Y.; Zheng, R. L. (2000) *Prog. Biochem. Biophys.* **27**:351-353.

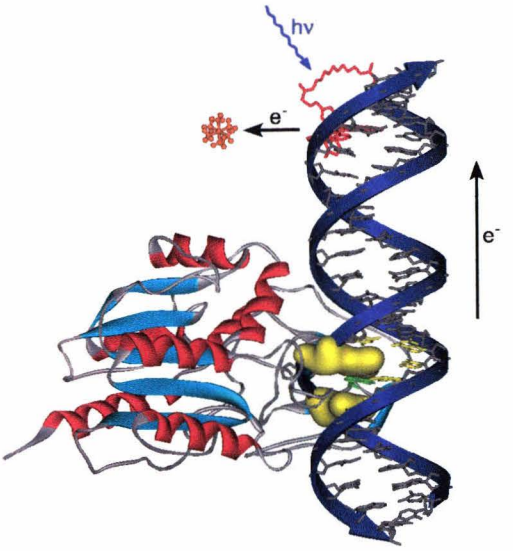

Figure 1. ***Cartoon depicting Flash-Quench Cycle induced DNA-CT on M. Ha I bound DNA. Adapted from Wagenknecht et al, 2001***

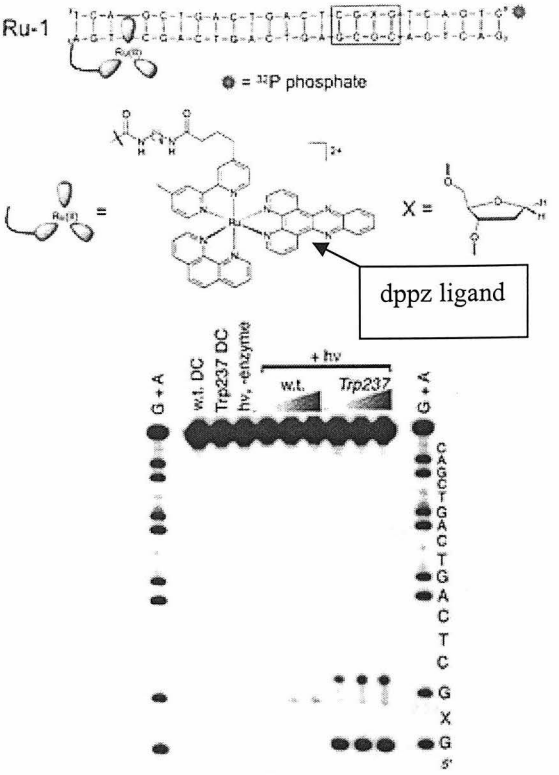

Figure 2. ***Gel depicting DNA damage due to DNA-CT through the site of trytophan intercalation into the DNA. Adapted from Wagenknecht et al, 2001***

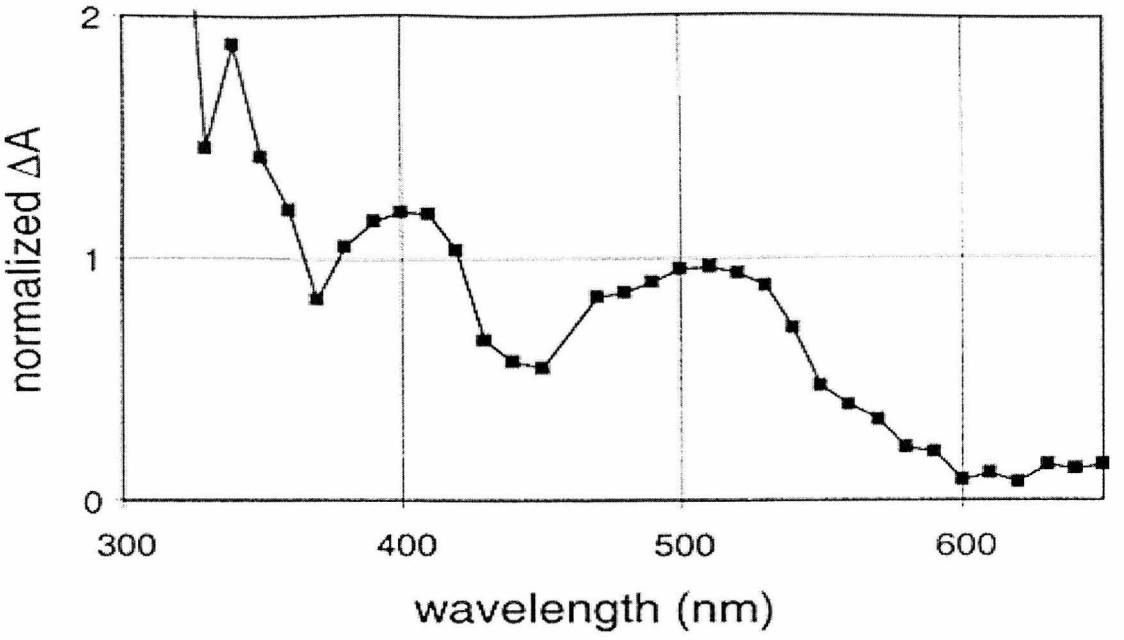

Figure 3. ***Transient absorption difference spectrum*** **. Depicts maxima for both guanine (390, 500) and tryptophan (510) radicals.** ***Adapted from Wagenknecht et al, 2001***

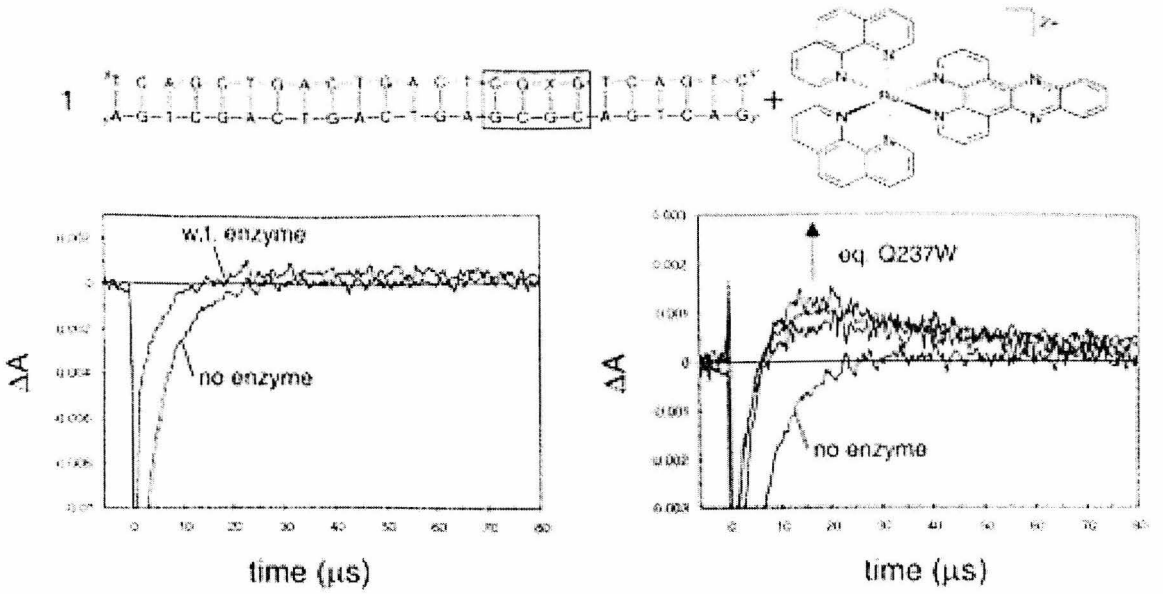

Figure 4. ***Transient absorption curves at 510nm.*** **These show the presence of increasing amounts of tryptophan radical with increasing equivalents of tryptophan mutant.** ***Adapted from Wagenknecht et al, 2001***

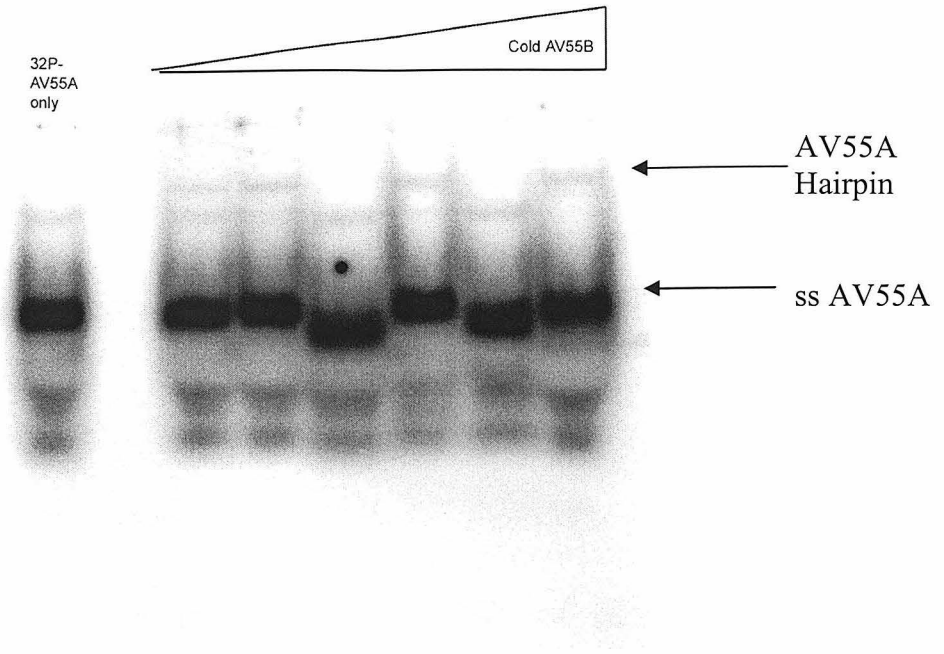

Figure 5. ***Attempted formation of dsDNA from ssAV55A and AV55B.*** **Strands were annealed by mixing in a 1:1 ratio, heating to 90 °C and cooling to 25 °C over 3 hours. AV55A was 5' labeled with 32P using T4 Poynucleotide Kinase (PNK)--standard protocol. Samples were loaded onto a 20% native PAGE gel and run for 10 hours at 200 V. Gel was pre-run for 2 hours at 200 V. Phosporimagery was used to visualize the gel. Exposure to phosphorimage screen was 15 hrs. The left lane is only AV55A. The other lanes are 250pM AV55A with titration of 250pM-500nM AV55B**

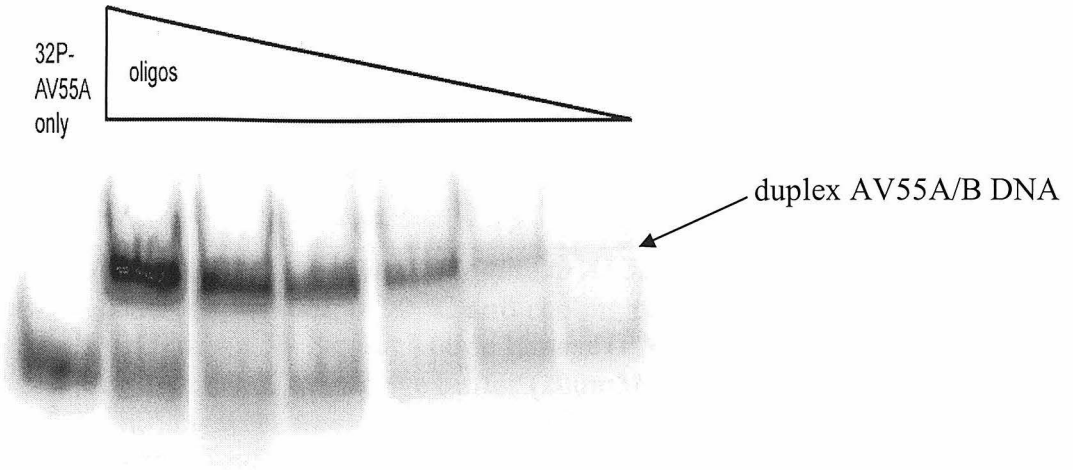

Figure 6. ***Formation of dsDNA from ssAV55A and AV55B.*** **Strands were annealed by mixing in a 1:1 ratio, heating to 90 °C and cooling to 25 °C over 3 hours. AV55A was 5' labeled with 32P using T4 Poynucleotide Kinase (PNK)--standard protocol. Samples were loaded onto a 20% native PAGE gel and run for 10 hours at 200 V. Gel was pre-run for 2 hours at 200 V. Phosporimagery was used to visualize the gel. Exposure to phosphorimage screen was 15 hrs. The left lane is only AV55A (15nM). The other lanes are range from 15-120nM in each AV55A an AV55B.**

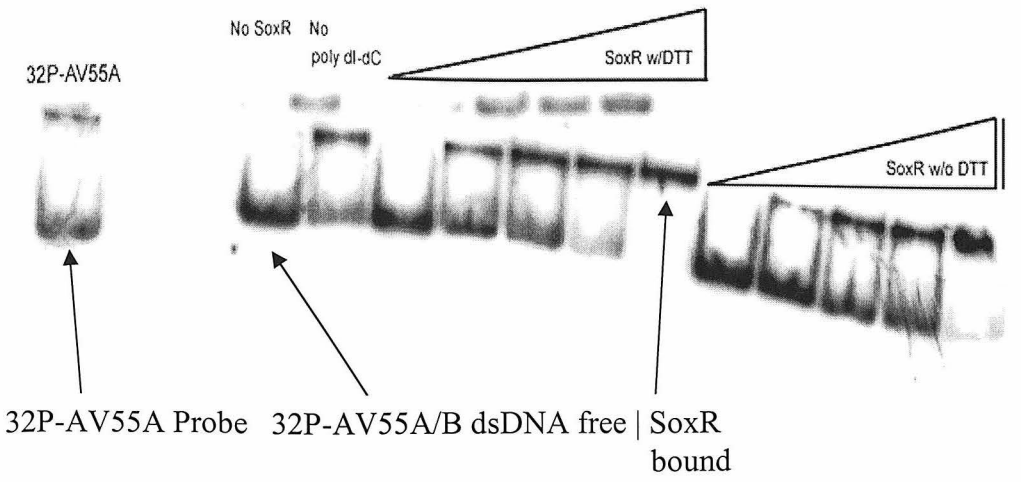

Figure 7. ***Gel Shift Analysis of SoxR-binding to AV55A/B.*** **. Strands were annealed by mixing in a 1:1 ratio, heating to 90 °C and cooling to 25 °C over 3 hours. AV55A was 5' labeled with 32P using T4 Poynucleotide Kinase (PNK)--standard protocol. SoxR, stored as 10μl aliquots at -86 °C in storage buffer (200mM KCl, 20mM MOPS), was defrosted at 4 °C. Serial dilutions were made in storage buffer, yielding 1-15 equivalents of AV55A/B (200nM) on which SoxR was to be bound. In each sample, SoxR was mixed with 1 x SoxR binding buffer and 32P-AV55A/B for 30 minutes at 25 °C. After the 30 minute preincubation period was up, samples were loaded onto a 10% native PAGE gel with concomitant application of current to minimize duration in wells. The gel(pre-run for 2 hrs at 200 V) was run for 2 hrs 15 min at 250 V. Phosporimagery was used to visualize the gel. Exposure to phosphorimage screen was 10 hrs. From left to right the lanes are as follows: 1, ssAV55A, 2, AV55A/B, No SoxR, 3, No poly dI-dC non-competetive inhibitor DNA, 4-8, 1-15 eq. of $SoxR_{dimer}$ w/DTT, 9-13, 1-15 eq. of $SoxR_{dimer}$ w/o DTT.**

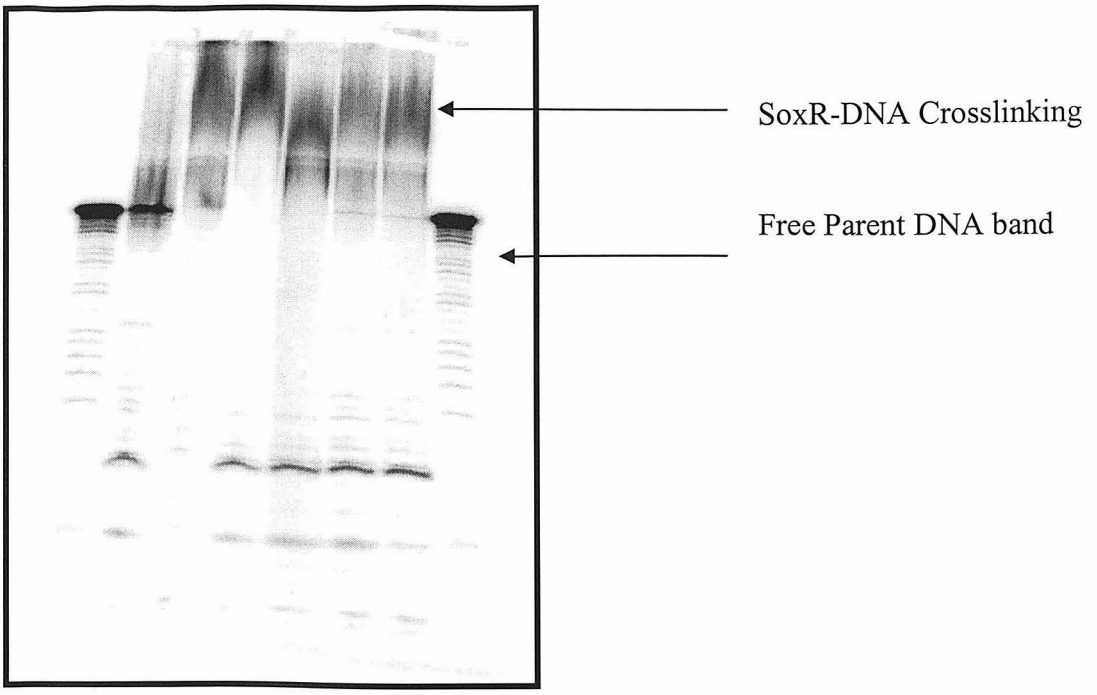

Figure 8. ***Representative gel of SoxR DNA photo-crosslinking during attempted flash -quench experiment.*** **$[SoxR]_{dimer}$=3μM, [32P-AV55A/B]= 200nM, $[Ru(phen)_2dppz]$ = 2μM, [Ru(NH3)6]= 5μM, 1 x SoxR binding buffer. 2nd lane from left has no SoxR, the 5 lanes following had SoxR. The first and last lanes were Maxam-Gilbert sequencing lanes(A+G) Irradiations were performed on a 1000 HgXe Arc Lamp with a monochromator for 30 min at a power of ~8mw. Typically, 20% DPAGE gels were run for 1 hr 15 min at 100 w and visualized by exposure to phosphorimage screens for 4-7 hrs.**

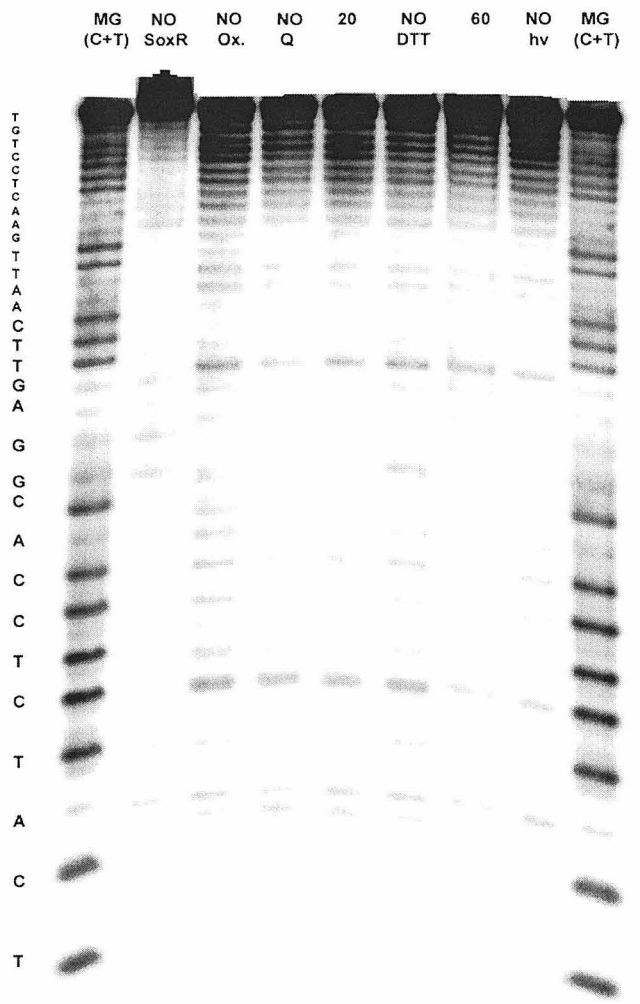

Figure 9. ***Representative gel of SoxR DNA Flash-Quench Experiments w.ith Proteinase K Treatment.*** **Same conditions as above except AV55B was radioactively labeled, not AV55A. Following irraditions, all samples were treated with 2μl 346μM Proteinae K and diluted to 400μl in proteinase K buffer (50 mM TRIS-Cl, 10mM $CaCl_2$, pH=7.6). Samples were heated to 55 °C for 1 hr, phenol/chloroform extracted, EtOH precipitated, dried and treated w/ 100μl 10% piperidine for 30 minutes at 90 °C. Samples were cooled and dried under vacuum, dissolved in denatuting loading dye and loaded onto, typically, 20% DPAGE gels (pre-run for 2 hrs at 100w), run for 1 hr 15 min at 100 w and visualized by exposure to phosphorimage screens for 4-7 hrs. From left to right, the lanes are as follows: Maxam-Gilbert Sequencing lane (C+T), AV55A/B only, No SoxR, No $Ru(phen)_2dppz$, No Ru(NH3)6, 20 minutes with everything, 60 minutes w/o DTT, 60 minutes with everything, No light, another Maxam-Gilbert Sequencing lane (C+T).**

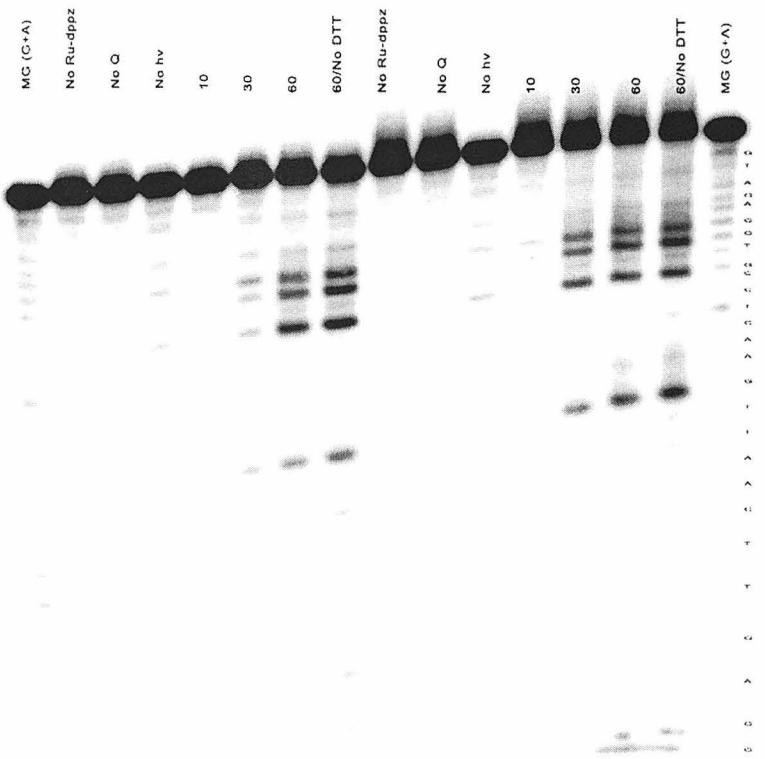

Figure 10. ***Flash Quench Under Optimized Conditions.*** **[32P-AV55A/B]= 1μM, [Ru(phen)$_2$dppz] = 3μM, [Ru(NH3)6]= 5mM, 1 x SoxR binding buffer. Irradiations performed using a HeCd laser at ~14mw for 60 min unless otherwise noted. From left to right, the lanes are as follows: Maxam-Gilbert Sequencing lane (C+T), No Ru(phen)2dppz, No Ru(NH3)6, No light, 10 min w/ everything, 30 min w/ everything, 60 min w/ everything, 60 min w/ everything except DTT, [Ru(NH3)6]= 100 μM for these experiments. The remaining lanes are a repeat of the first set using 500 μM Ru(NH3)6. Gel conditions and visualization same as above.**

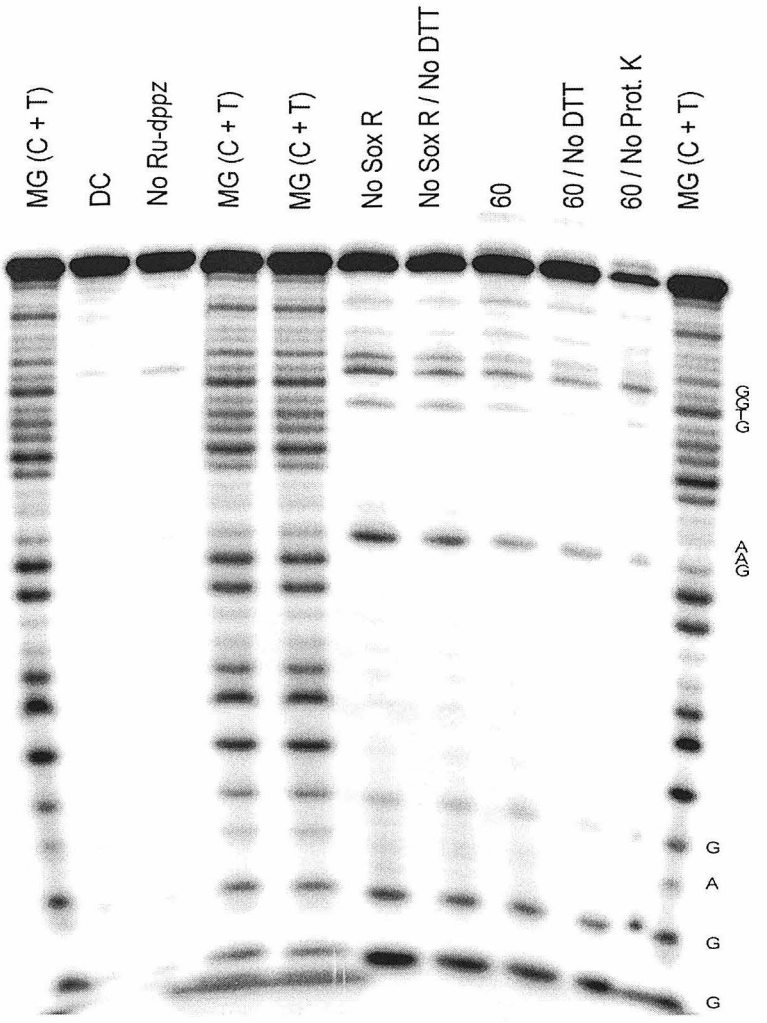

Figure 11. ***SoxR-DNA Flash Quench Experiment with Optimized Conditions.*** **$[SoxR]_{dimer}$=12μM, [32P-AV55A/B]= 1μM, $[Ru(phen)_2dppz]$ = 3μM, [Ru(NH3)6]= 5mM, 1 x SoxR binding buffer. Irradiations performed using a HeCd laser at ~14mw for 60 min. Sample preparation/SoxR binding same as in Fig. 9 above. Purification and gel conditions also same as above. From left to right, the lanes are as follows: Maxam-Gilbert Sequencing lane (C+T), No light, No $Ru(phen)_2dppz$, 2 additional MG sequencing lanes, AV55A/B only (No SoxR), AV55A/B only (No SoxR. No DTT), Everything w/DTT, Everything except DTT, Everything w/o post-proteinase K treatment, MG sequencing lane (C+T)**

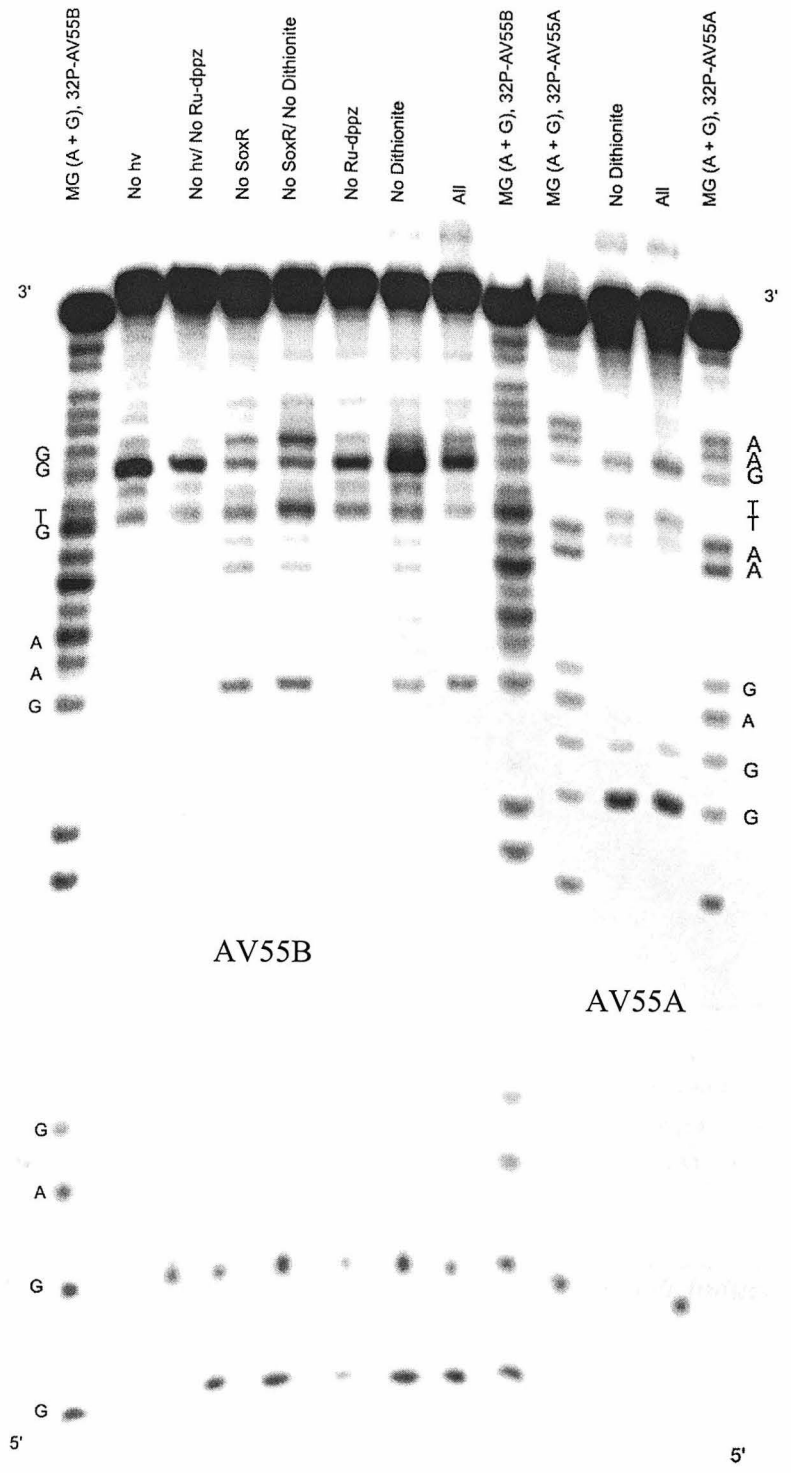

Figure 12. ***SoxR$_{red}$-DNA Flash Quench Experiment with Optimized Conditions.*** **Conditions same as above except 32P-AV55A/B was co-incubated with SoxR and 2mM Dithionite. From left to right, lanes are self-explanatory by analogy with other gels. The four farthest lanes represent two experiments performed on 32P-AV55A duplexed with cold AV55B.**

AV 55A *5′-AGTCATCTCCACGGAGTTCAATTGAACTCCTGT-3
AV 55B 3′-TCAGTAGAGGTGCCTCAAGTTAACTTGAGGACA-5′*

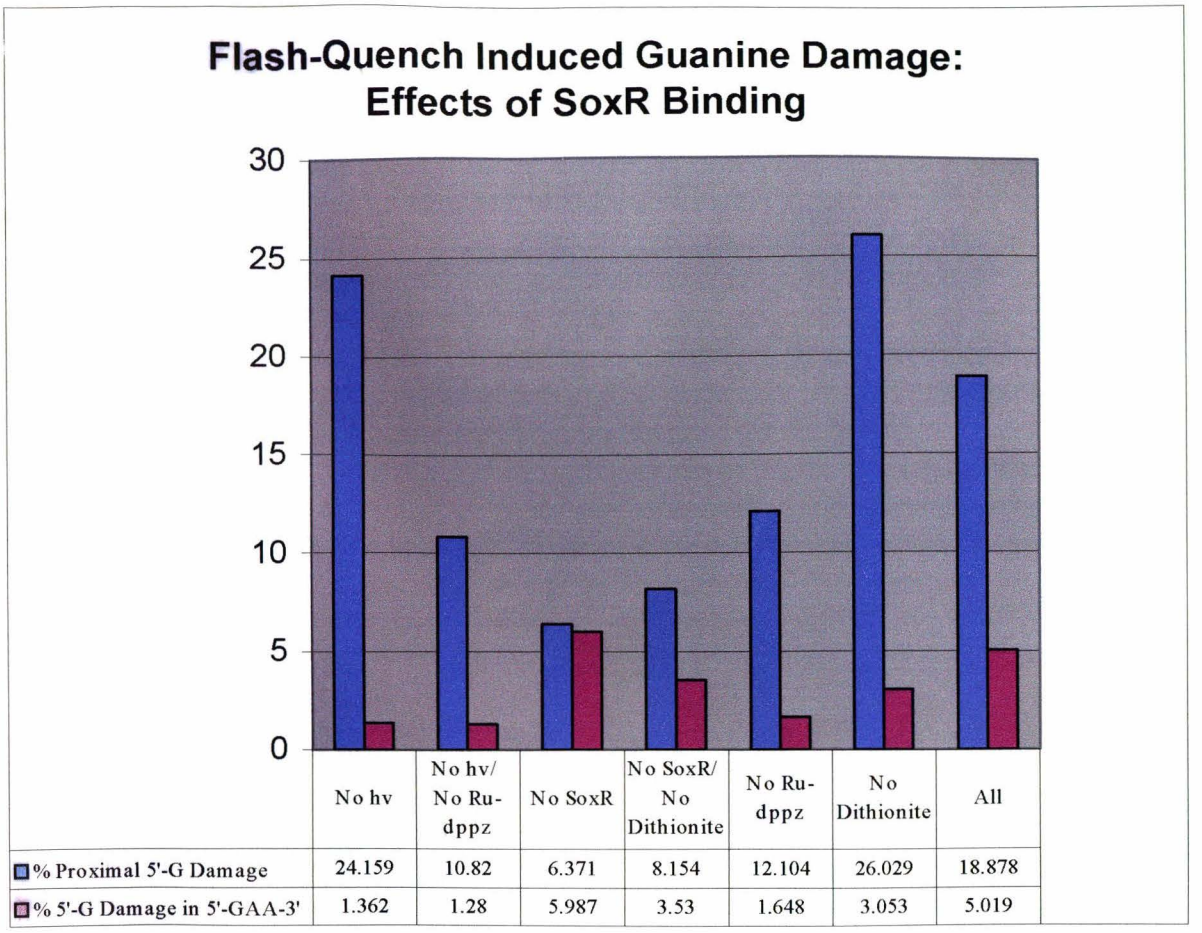

	No hv	No hv/ No Ru-dppz	No SoxR	No SoxR/ No Dithionite	No Ru-dppz	No Dithionite	All
% Proximal 5'-G Damage	24.159	10.82	6.371	8.154	12.104	26.029	18.878
% 5'-G Damage in 5'-GAA-3'	1.362	1.28	5.987	3.53	1.648	3.053	5.019

Figure 13. ***Effects of SoxR binding on Flash Quench Induced Guanine Damage***

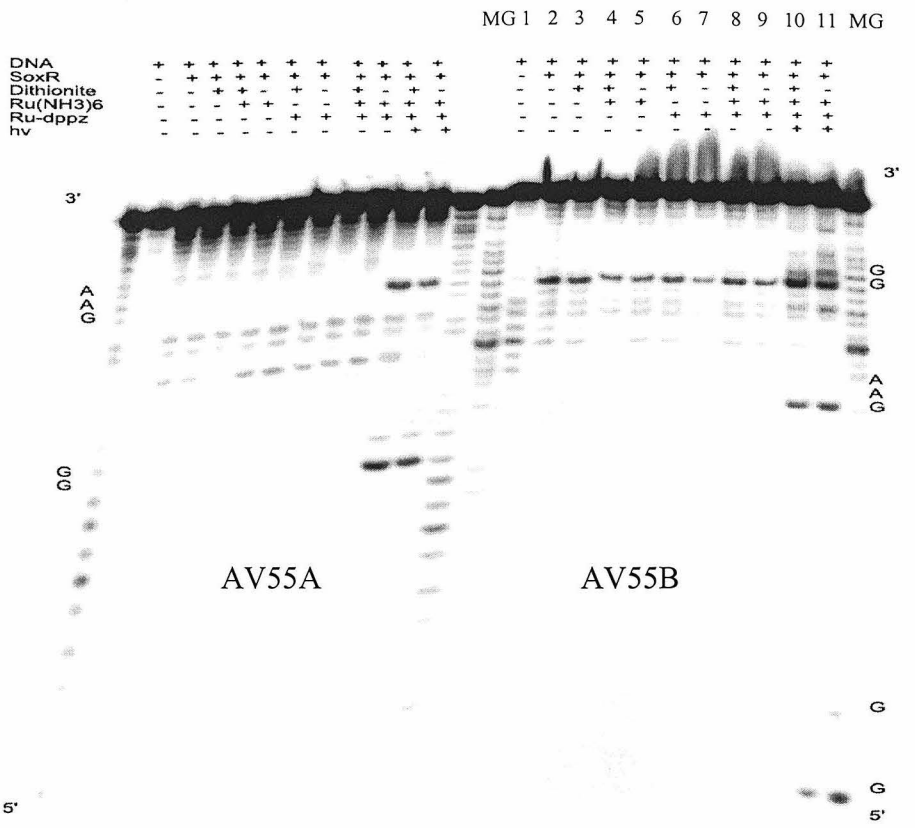

Figure 14. ***Selective Oxidation Upon SoxR Binding under non-FQ conditions at a 5'G of a 5'-GG-3' Site located Outside the SoxR binding site.***

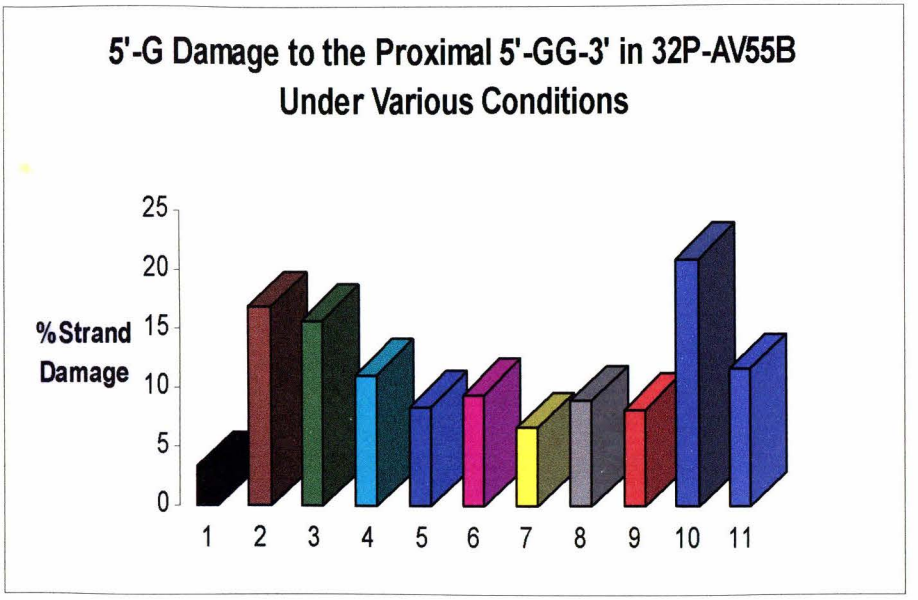

Figure 15. ***% Overall Strand Damage at the Selectively Oxidized 5'-GG-3'shown in Fig. 14.***

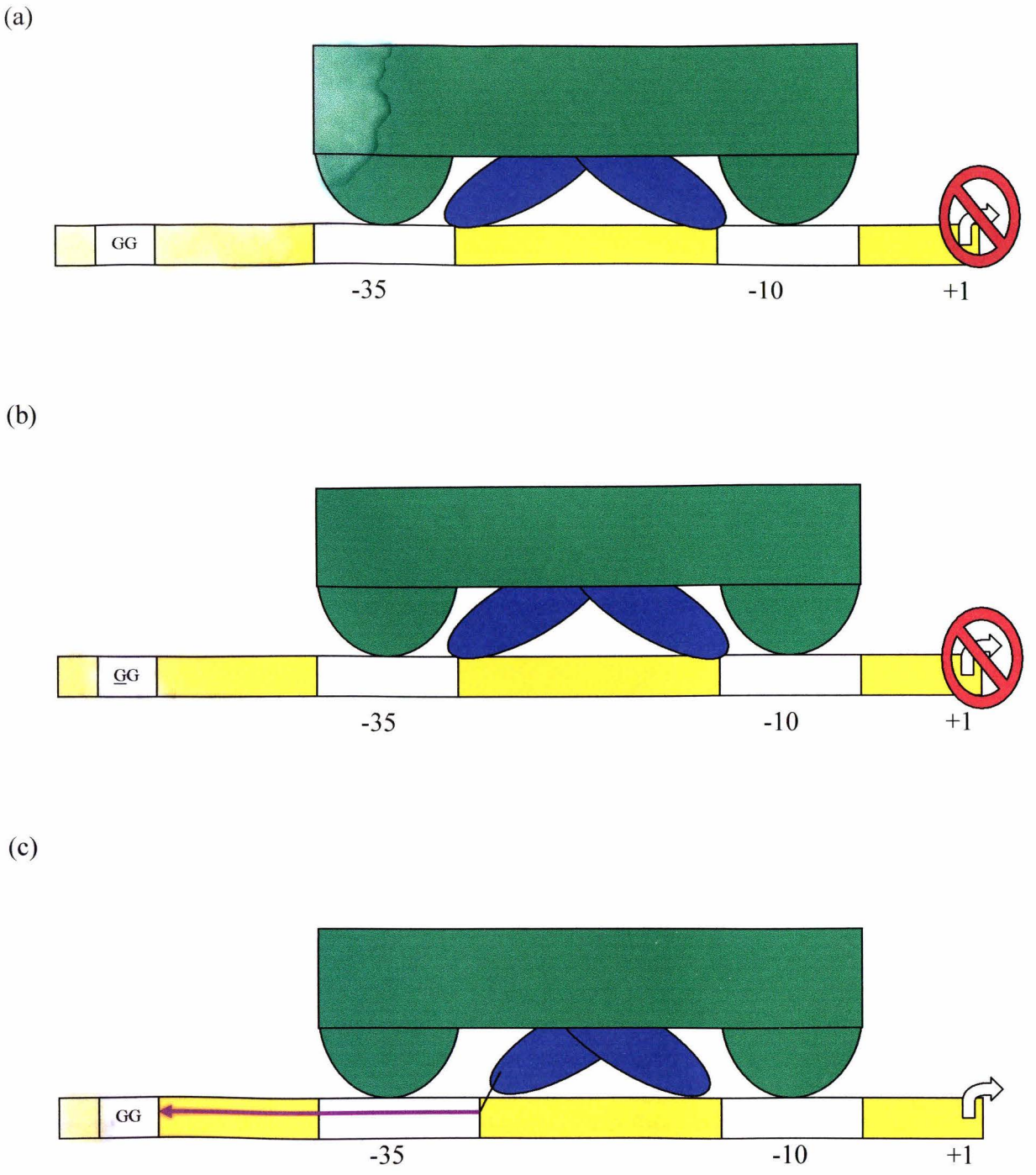

Figure 16. ***Current Model For SoxR Biosensing/Autooxidation Mechanism.*** **(a) Basal Conditions. SoxR is reduced (b) Oxidative Stress. 5'-GG-3' is oxidized to a $G^{\cdot+}$ (c) SoxR reduces the $G^{\cdot+}$, autooxidizing in the process. SoxS is transcribed. In the cartoon, RNA pol is in green, SoxR is in blue, the white and yellow strip represents the soxS promoter. The "GG" depicts the guanine doublet found 15 bp upstream from the end of the palidromic SoxR binding site.**

(a)

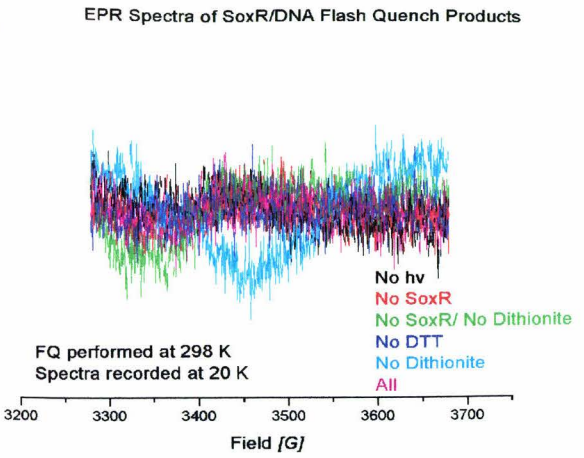

(b)

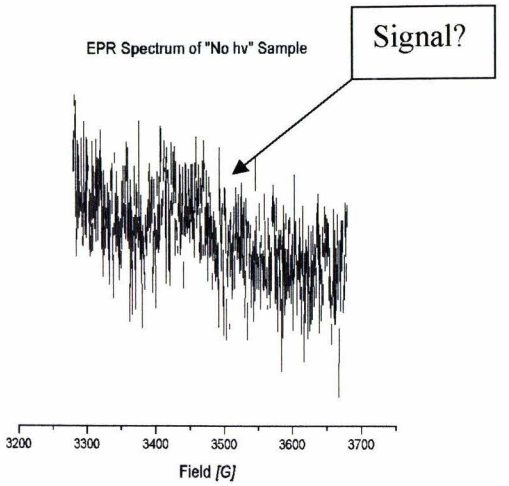

Figure 17. ***EPR spectra of SoxR-DNA FQ reaction.*** **(a) Cold AV55A/B was used for these experiments. The distinctions are self explanatory (b) Sprectrum of "No hv" sample.**

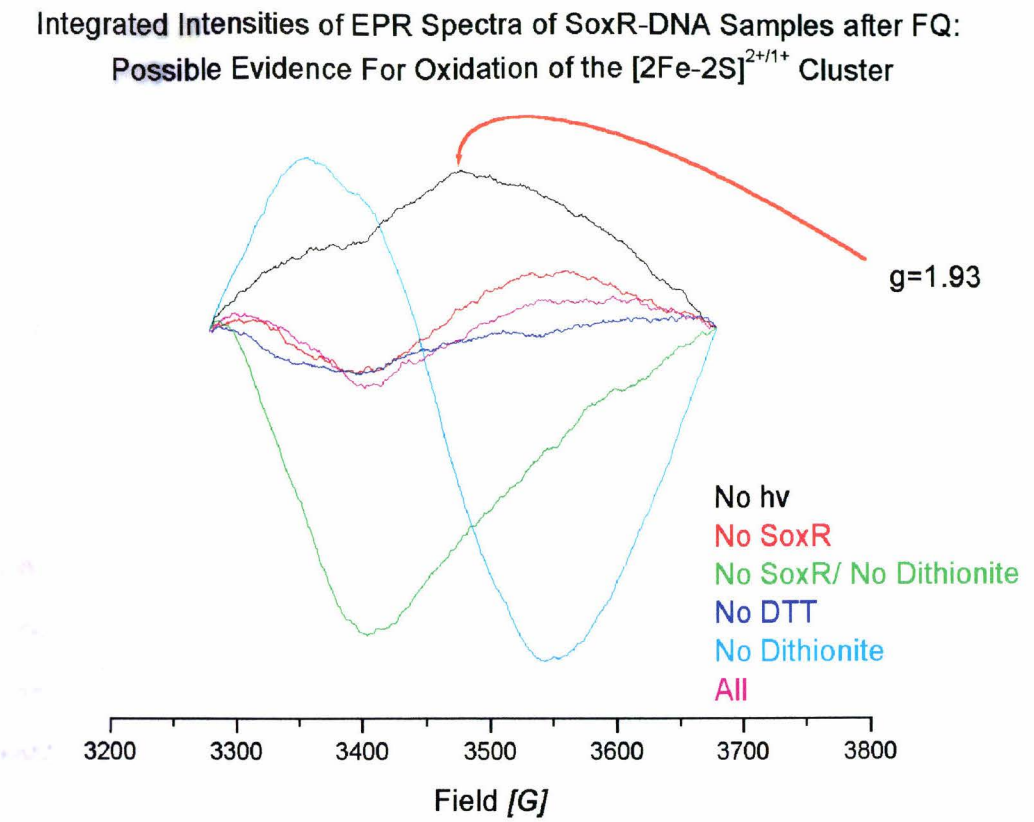

Figure 18. ***Integrated Intensities of EPR spectra shown in Fig. 18.***

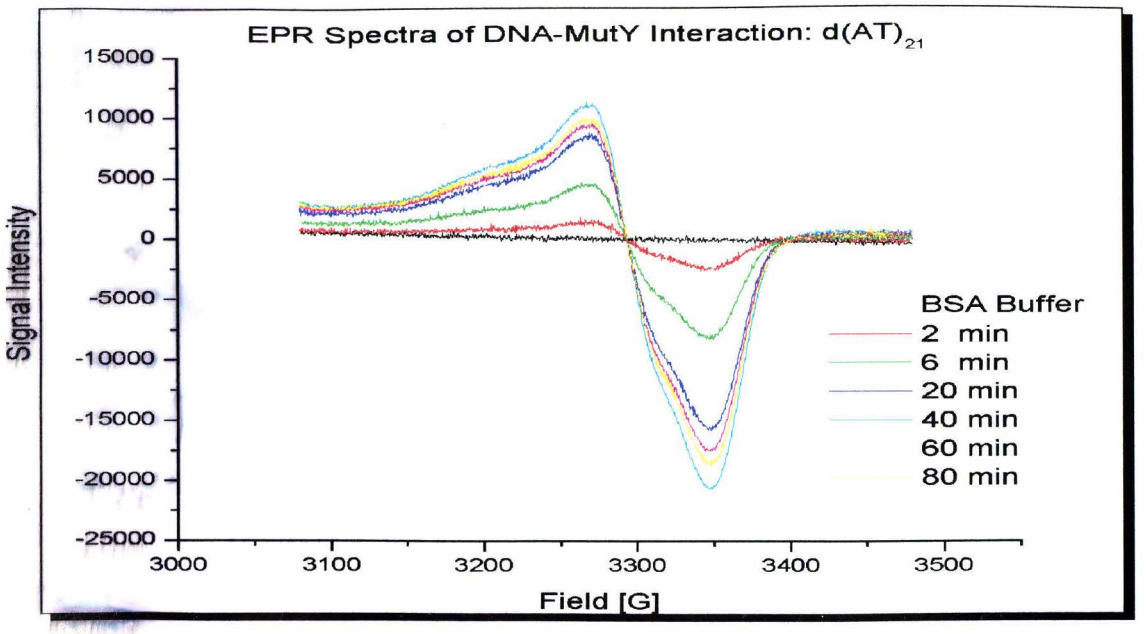

Figure 19. ***EPR spectra from the MutY- All AT oligo interaction over time.*** **The reaction buffer is 10mM NaCl, 20mM TRIS-Cl, pH 7.5 and contains .1mg/mL acetylated bovine serum albumin (BSA).**

All AT oligo:

5'-ATATATATATATATATATATA-3'
3'-TATATATATATATATATATAT-5'

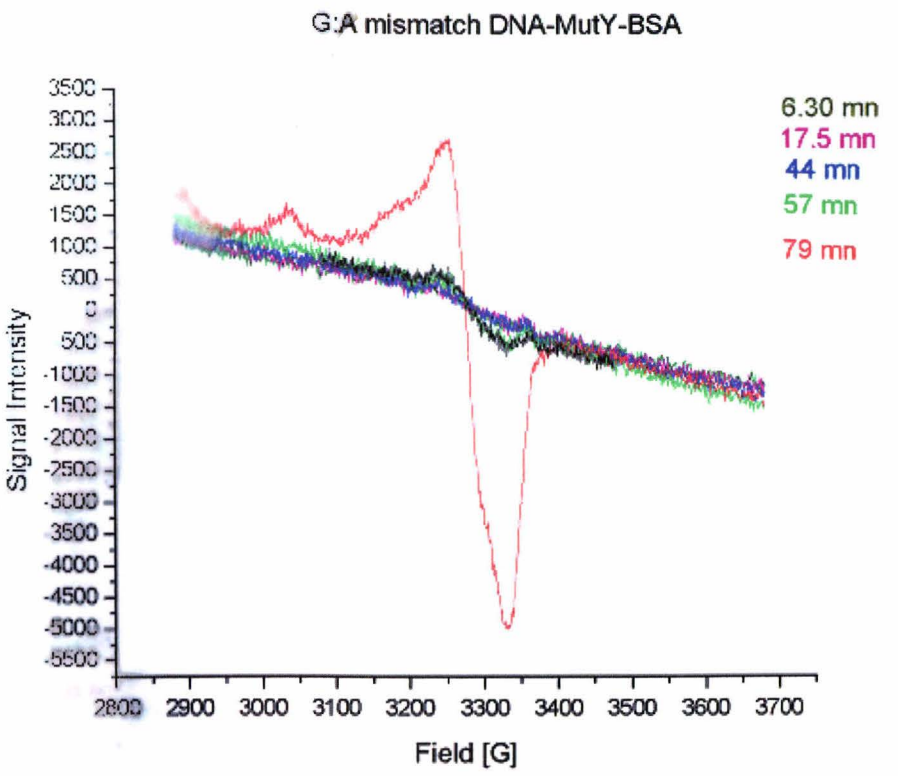

Figure 20. ***EPR spectra from the MutY- G:A mismatch oligo interaction over time.*** **Other Conditions same as in Fig. 19.**

G:A mismatch oligo:

5'-ATATATAGATATATATATATA-3'
3'-TATATATATATATATATATAT-5

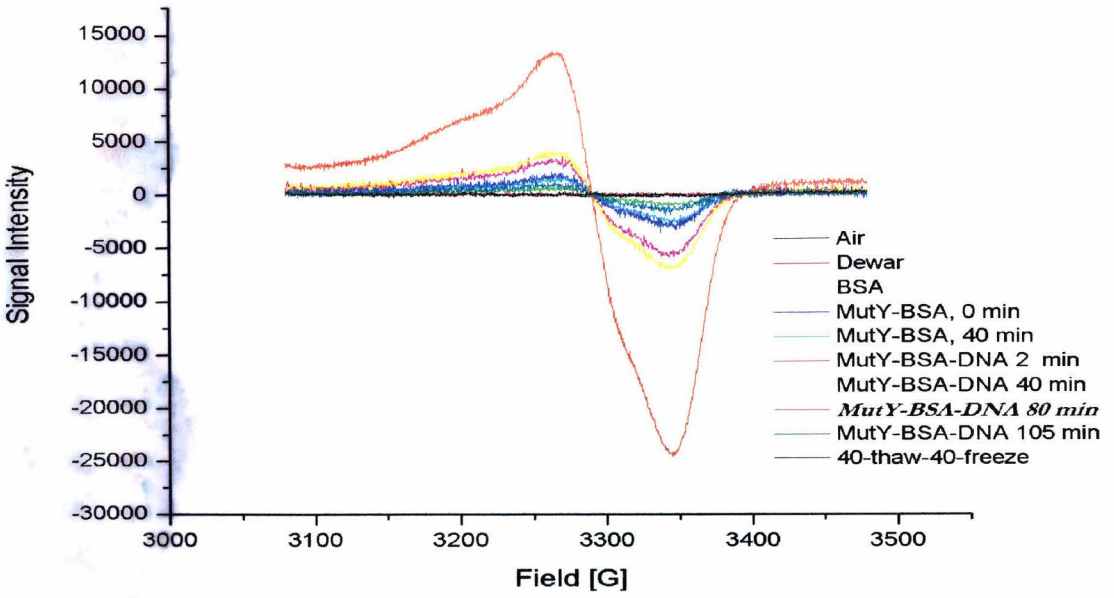

Figure 21. ***Same type experiment as that performed in Figure 20.***

(a)

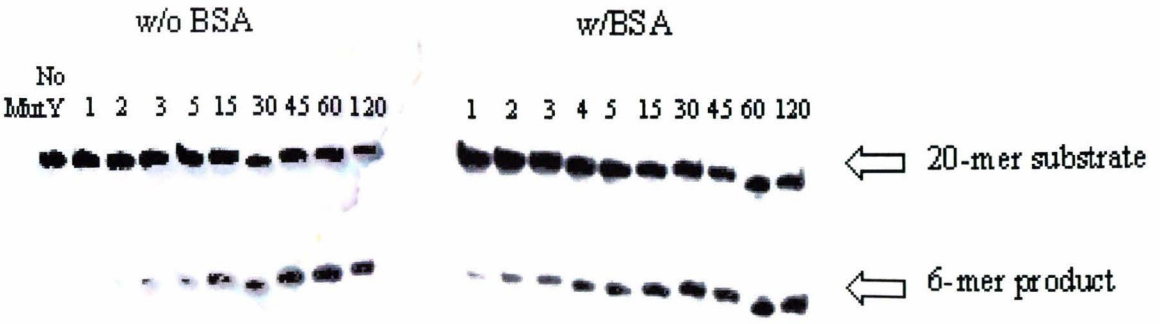

(b)

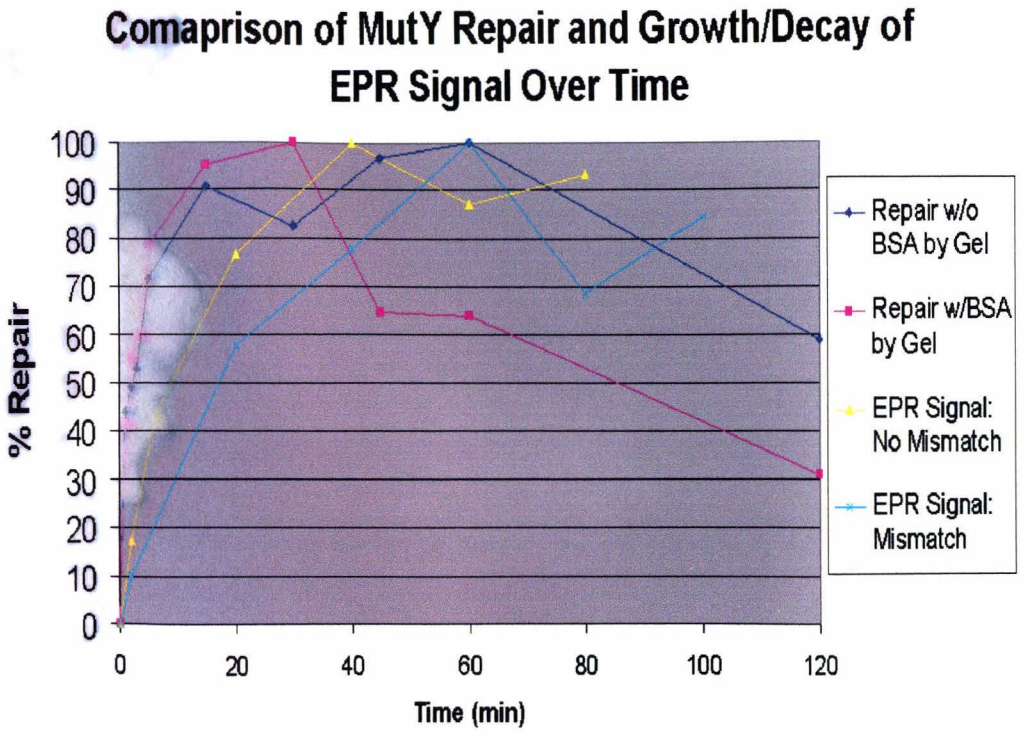

Figure 22. ***MutY Adenine Glycosylase Activity and EPR Signal Growth*** **(a) Adenine Glycosylase activity using MutY. Numbers represent time (min) reaction was stopped after inital mixing of MutY with G:A mismatch oligo substrate (b) EPR signal gowth and MutY repair curves (based on Fig. 22a) were normalized to their respective max and co-plotted on the same time scale.**

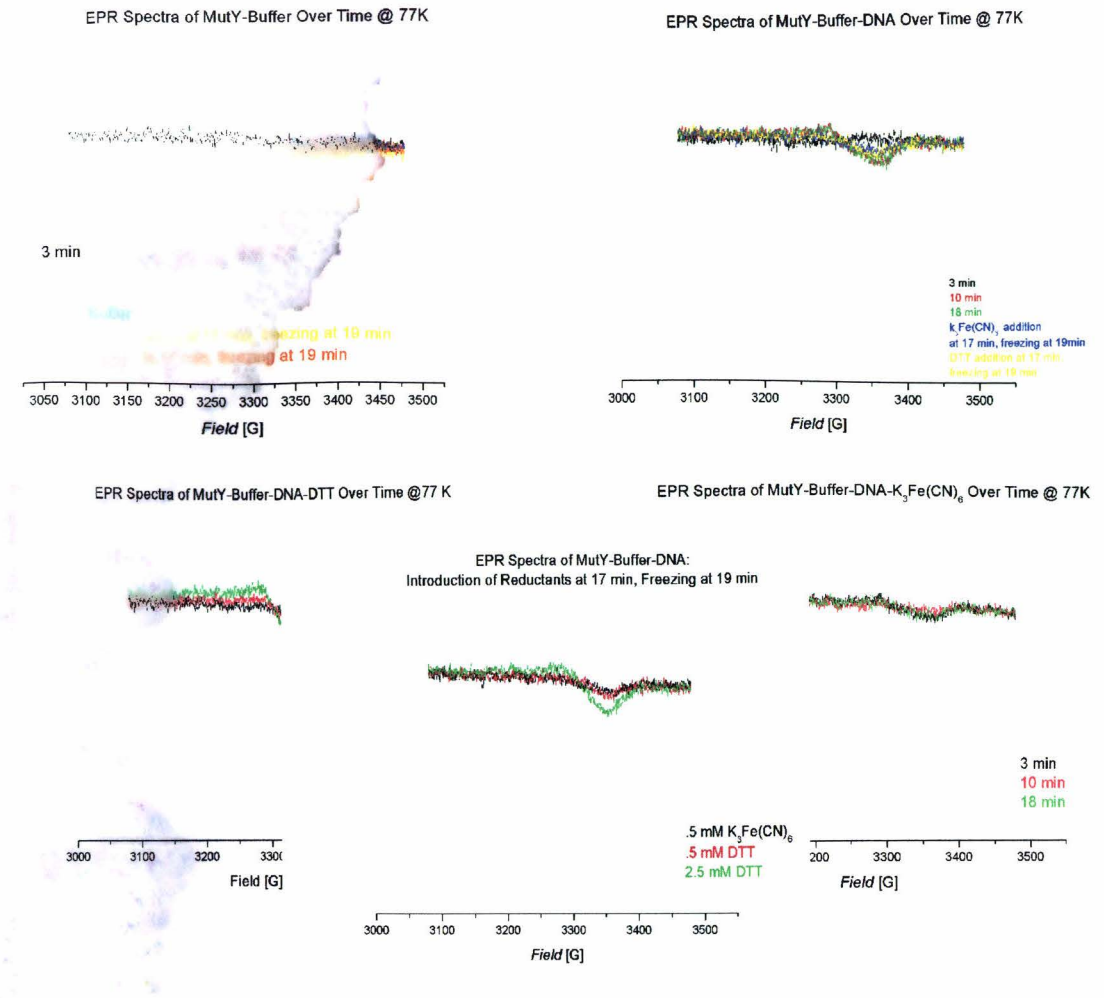

Figure 23. ***Effects of oxidants and reductants on EPR spectra of MutY-DNA interaction***

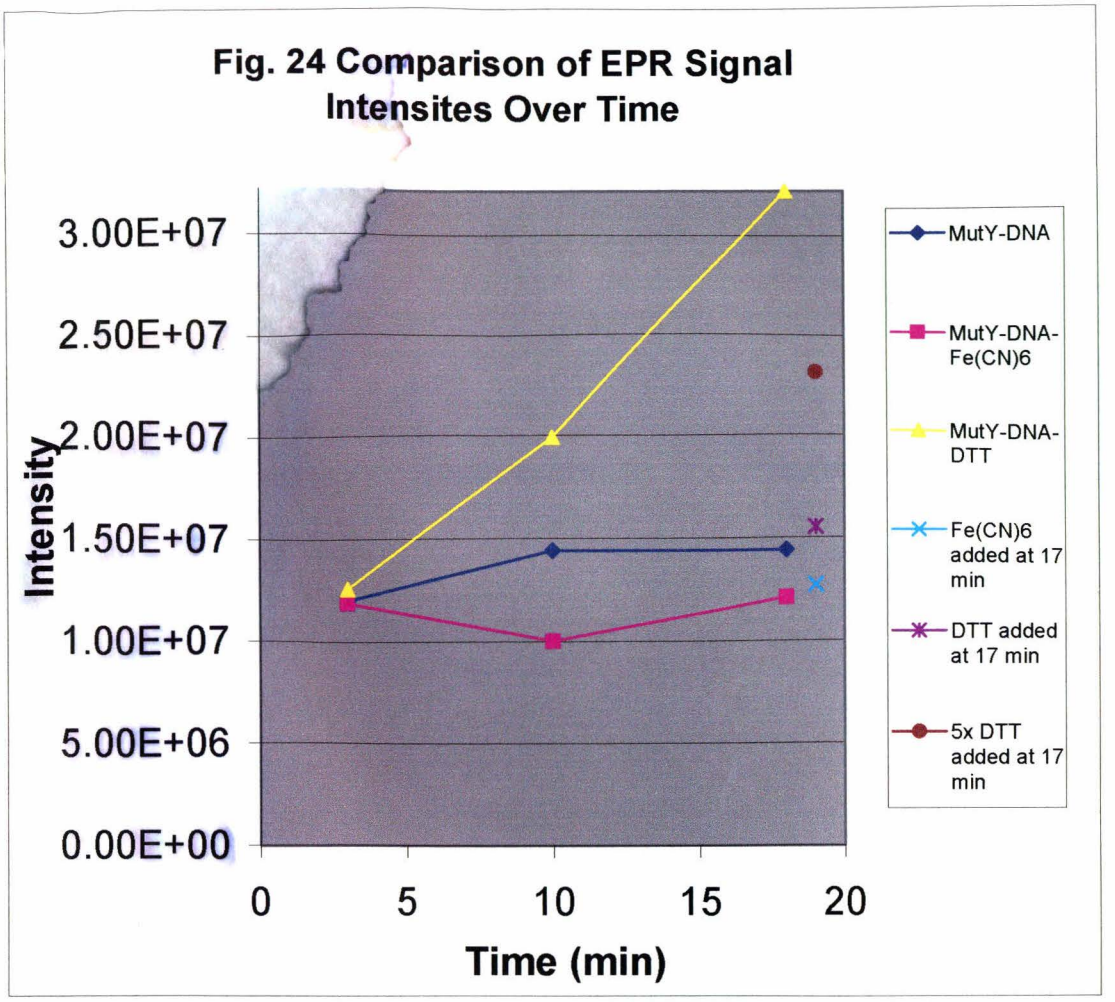

Figure 24. ***Comparison of EPR signal Intensities from Fig. 23***

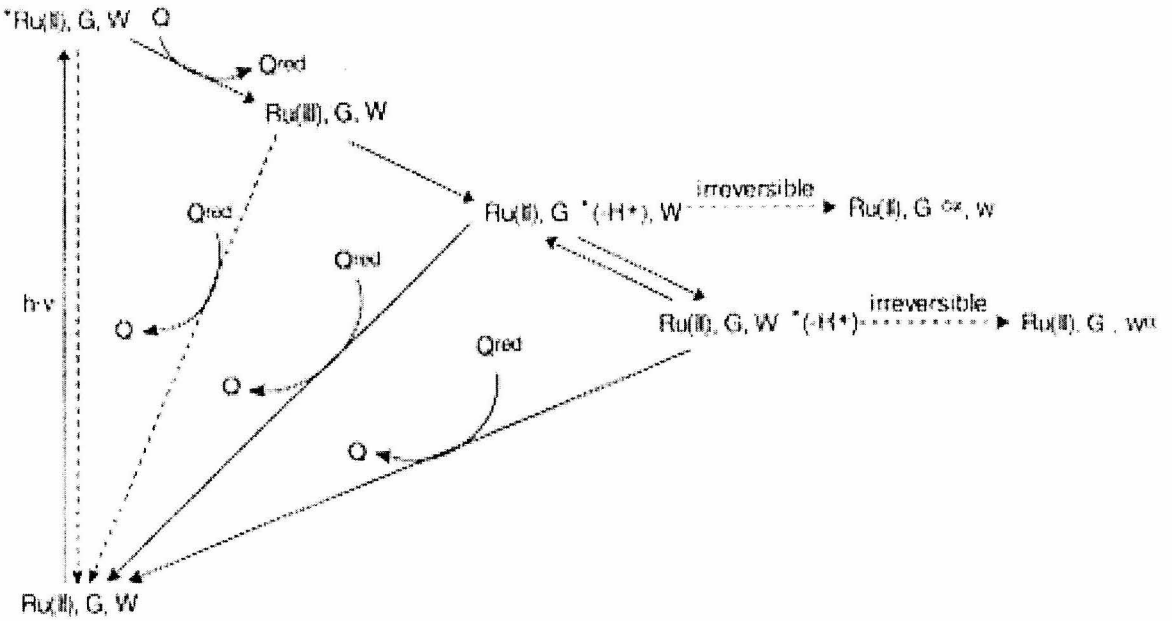

Scheme 1. The Flash Quench Cycle

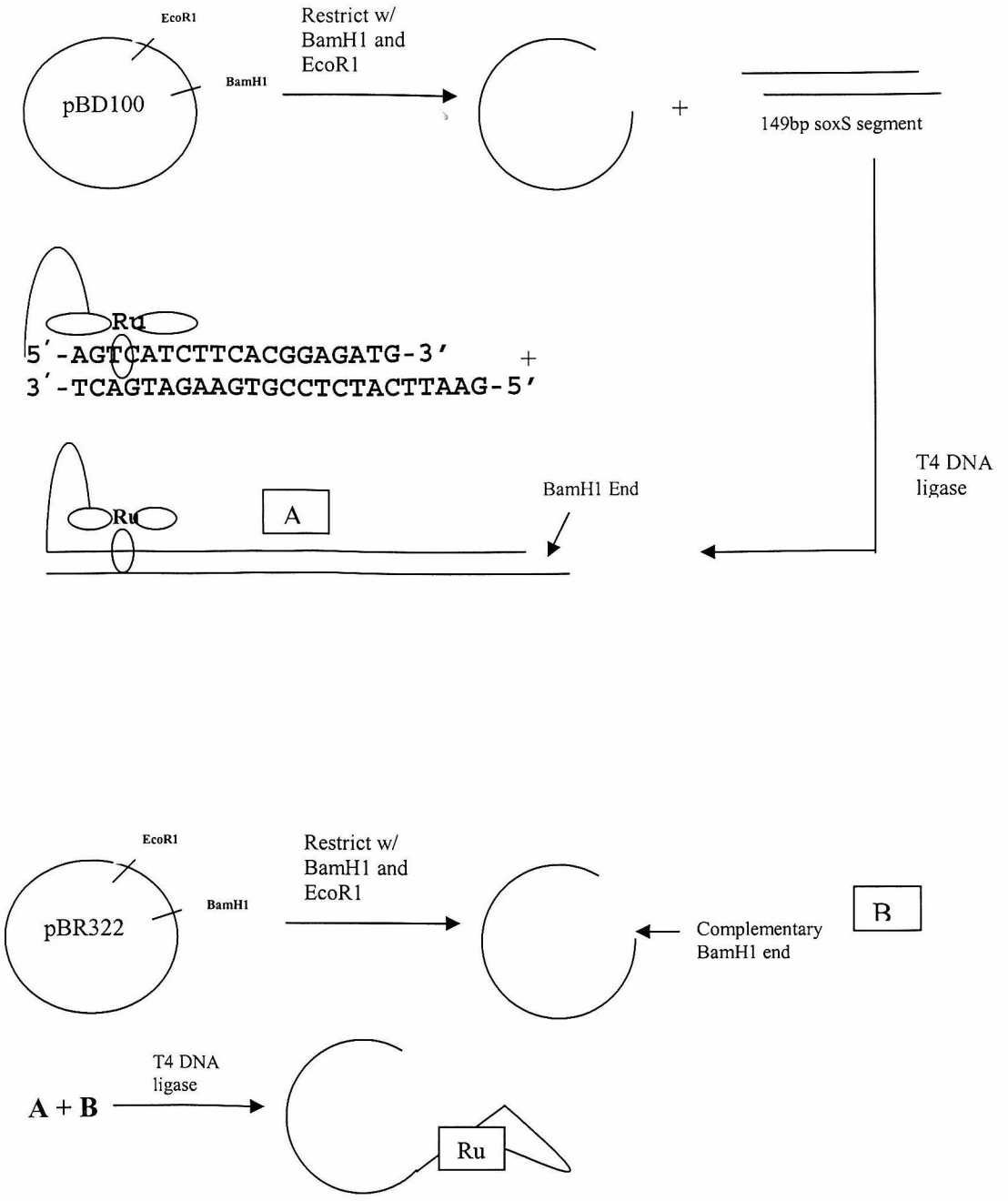

Scheme 2. ***Construction of covalently tethered Ru(phen)(bipy')dppz^{2+} to a soxS promoter containing plasmid.***